UNIVERSITY OF CALIFORNIA, SAN DIEGO

Modeling and Online Parameter Identification Methods for Electrohydraulic Valvetrain Systems

A Thesis submitted in partial satisfaction of the
requirements for the degree Master of Science

in

Engineering Sciences (Mechanical Engineering)

by

James Gray

Committee in charge:

Professor Miroslav Krstić, Chair
Professor Robert R. Bitmead
Professor Jorge Cortés

2009

The Thesis of James Gray is approved, and it is acceptable in quality and form for publication on microfilm and electronically:

_____

_____

_____

Chair

University of California, San Diego

2009

To my parents,
who don't understand exactly what I do
but support me every minute I do it

TABLE OF CONTENTS

LIST OF FIGURES

LIST OF TABLES

ACKNOWLEDGEMENTS

This thesis is the product of the work and support of many people that I would like to thank. Firstly, I would like to express my gratitude to my advisor Professor Miroslav Krstić for the opportunity for this research project, his excellent advice and guidance throughout the research project. His encouragement led me to pursue the field of control systems.

I would like to thank my parents Timothy and Teresita, my sisters Kathleen and Megan, and my brother William for all the love and encouragement throughout the years. They provided a solid foundation to build upon without which I would not be where I am today.

I would like to thank Nalin Chaturvedi, Sungbae Park, Aleksandar Kojic, and Karsten Mischker from Bosch. They provided the motivation and opportunity for the research, as well as the financial support. The time they spent with us over many teleconferences and flying to UCSD to go over the project is invaluable.

I would like to thank the members of my committee for their helpful questions and comments, and lending their time and expertise to this project.

I would like to thank my fellow graduate students, Nima Ghods, Paul Frihauf, Antranik Siranosian, Jennie Cochran, Joe Doblack, David Zhang, Andrew Kwok, Gabe Graham, James Krieger, Alicia Powers, Nikos Berkiaris-Liberis, Halil Basturk, and Gideon Prior for creating an enjoyable and collaborative research environment. A special thanks goes to Nima and Paul for all their advice and answers to my constant inquiries.

Lastly, I would like to give a large thanks to Ihui Wu for being a great friend, a source of unending encouragement, and an understanding mind.

Chapter 1, in part, is an adaptation of the paper by J. Gray, M. Krstic, N. Chaturvedi, P. Sungbae, A. Kojic, K. Mischker "Parameter Identification for Electro-hydaulic Valvetrain Systems," which was submitted to the *ASME Journal of Dynamic Systems, Measurement and Control*.

Chapter 2, in part, is an adaptation of the paper by J. Gray, M. Krstic, N. Chaturvedi, P. Sungbae, A. Kojic, K. Mischker "Parameter Identification for Electro-hydaulic Valvetrain Systems," which was submitted to the *ASME Journal of Dynamic*

Systems, Measurement and Control.

Chapter 3, in part, is an adaptation of the paper by J. Gray, M. Krstic, N. Chaturvedi, P. Sungbae, A. Kojic, K. Mischker "Parameter Identification for Electro-hydaulic Valvetrain Systems," which was submitted to the *ASME Journal of Dynamic Systems, Measurement and Control*.

Chapter 4, in part, is an adaptation of the paper by J. Gray, M. Krstic, N. Chaturvedi, P. Sungbae, A. Kojic, K. Mischker "Parameter Identification for Electro-hydaulic Valvetrain Systems," which was submitted to the *ASME Journal of Dynamic Systems, Measurement and Control*.

Chapter 5, in part, is an adaptation of the paper by J. Gray, M. Krstic, N. Chaturvedi, P. Sungbae, A. Kojic, K. Mischker "Parameter Identification for Electro-hydaulic Valvetrain Systems," which was submitted to the *ASME Journal of Dynamic Systems, Measurement and Control*.

VITA

2007	Bachelor of Science in Mechanical Engineering, University of California, San Diego
2007-2008	Teaching Assistant, Department of Mechanical Engineering, University of California, San Diego
2009	Master of Science in Engineering Sciences (Mechanical Engineering), University of California, San Diego

PUBLICATIONS

J. Gray, M. Krstic, N. Chaturvedi, P. Sungbae, A. Kojic, K. Mischker "Parameter Identification for Electrohydaulic Valvetrain Systems," submitted to the *ASME Journal of Dynamic Systems, Measurement and Control*.

ABSTRACT OF THE THESIS

Modeling and Online Parameter Identification Methods for Electrohydraulic Valvetrain Systems

by

James Gray
Master of Science in Engineering Sciences (Mechanical Engineering)
University of California San Diego, 2009
Professor Miroslav Krstić, Chair

We consider an Electrohydraulic Valve System (EHVS) model with uncertain parameters that may possibly vary with time. This is a nonlinear third order system consisting of two clearly separated subsystems, one for piston position and the other for the chamber pressure. The nonlinearities involved are flow-pressure characteristics of the solenoid valves, the pressure dynamics of the chamber due to varying volume, and a variable damping nonlinearity. We develop a parametric model that is linear in the unknown parameters of the system using filtering. We deal with a nonlinear parameterization in the variable damping term using the Taylor approximation. We design two parameter identifiers which employs either a continuous-time unnormalized least-squares update law with a forgetting factor or a gradient update law. These update laws exponentially converges to the true parameters under a persistence of excitation condition, which is satisfied due to the periodic regime of operation of EHVS. We present simulation results that show good following of unknown parameters even with the presence of sensor noise. We also create a hybrid model of the EHVS and apply the identifiers. In the presence of the unmodelled dynamics we find there remains good following of the unknown parameters.

1

Introduction

There is a continuous push to improve the operation of internal combustion engines. Increasing power per mass or volume, increasing operating efficiency, and decreasing emissions are a few areas which are important improvements in an engine operation. Variable valve timing (VVT) is a technological improvement which achieves the aforementioned improvements. Normally, internal combustion engines use valves timed by cams rotating on a camshaft to allow intake of fuel and exhaust of the waste. However, the profiles of the cams are optimized for certain engine speeds. Because the valve timings are constrained to the motion of the camshaft, operation at other speeds results in lower fuel efficiency, higher emissions, and reduced torque performance. VVT systems seek to achieve optimum intake and exhaust at each engine speed.

Even with a camshaft, there are VVT strategies that can improve fuel economy at partial load. [10] investigate a simple variable cam phaser as a VVT strategy. A variable cam phaser has the ability to shift the camshaft to retarded positions. This valve timing variation proves itself to be an effective means of reducing specific fuel consumption at partial load by reducing pumping losses. Work has been done by [23] to optimize the spark timing and valve openings to achieve minimum fuel consumption via extremum seeking. A method of both VVT and variable valve lift using a modified camshaft has been explored in [16]. The addition of variable lift has been shown to improve low-end-torque and maximum power. This method, using the appropriate cam profiles, can achieve precise variable valve lift mechanically. Variable

valve lift, coupled with a VVT scheme, offers even more improvement to engine operation. Moving away from the camshaft allows even greater control and cycle to cycle optimization of the valve train. The electro-hydraulic valvetrain system (EHVS) developed by Bosch is one of the most flexible options for variable valve timing in automotive engines.

1.1 What is the EHVS?

Hydraulic actuators are used throughout industry in a wide number of applications. With a small size and a high force-to-mass ratio the actuators have found applications in electro-hydraulic positioning [9], flight control surfaces [18], and active suspension control in automobiles [1]. Given the proven controllability, reliability and force-to-mass ratio, a hydraulic system is a good replacement of the camshaft to time and control lift of the valves.

EHVS is one of the most flexible options because EHVS valve timings are fully independent of the crankshaft position. This flexibility allows cycle-to-cycle control of fuel intake and waste exhaust which leads to the previously mentioned benefits. Additionally, at low-to-moderate engine speeds, the timing can be optimized to improve full load torque as discussed by [7]. To further add to the flexibility both gasoline engines and Diesel engines can be fitted with the valve system. Figure 1.1 shows the Diesel engine actuator V0.5 on the left and the gasoline engine actuator V0.7 on the right. Both valves can cover the entire engine's (either Diesel or gasoline) operating range, can be assembled individually on the engine, and stand alone tests of the cylinder head are possible. In addition actuator V0.7 uses common engine valves and has a variable valve brake to achieve soft seating of the valve.

An example of the complete EHVS actuation scheme on a four cylinder/sixteen valve gasoline engine can be seen in Figure 1.2. This configuration has been tested on an engine test bed since the end of 2002. [7] found benefits including: fuel savings of up to 20% on automobiles, a decrease in emissions such as NO_x, and torque improvements at low speeds. Chapter 3 will discuss in detail the operation and model of the EHV System.

Figure 1.1: Two variations of the EHVS actuator [7]

1.2 Important Degrees of Freedom in EHVS

According to [7] there are many important degrees of freedom in EHVS when compared to a camshaft driven valvetrain. The new options available to EHVS are comprised of modifications in the exhaust cycle, intake cycle, and hydraulic system.

The following is a summary of the events and the associated benefits achieved from modifying them. The aim of the exhaust opening parameter is the optimization of the high pressure process by minimizing the expansion losses in the area of the bottom dead center. The exhaust valve lift is a compromise on hydraulic dissipation minimization by means of reduced lift and exhaust work and the internal residual gas recirculation. The last exhaust event, the valve closing, is important in the setting and control of the residual gas content in the cylinder at part load and optimizing scavenging at full load.

Having intake control with EHVS provides the ability for optimization in the same three events, opening, closing, and valve lift as the exhaust cycle. Though the intake opening event has a similar purpose as the exhaust closing, mainly setting the residual gas content in the cylinder at part load and optimizing scavenging at full load, the intake closing and valve lift events offer different optimization options. The setting of intake closing is required for setting the load at part load and necessary for optimizing volumetric efficiency and the torque drop-off rate at full load. The valve lift of the intake is the major fuel consumption factor of the engine at part load. At part load

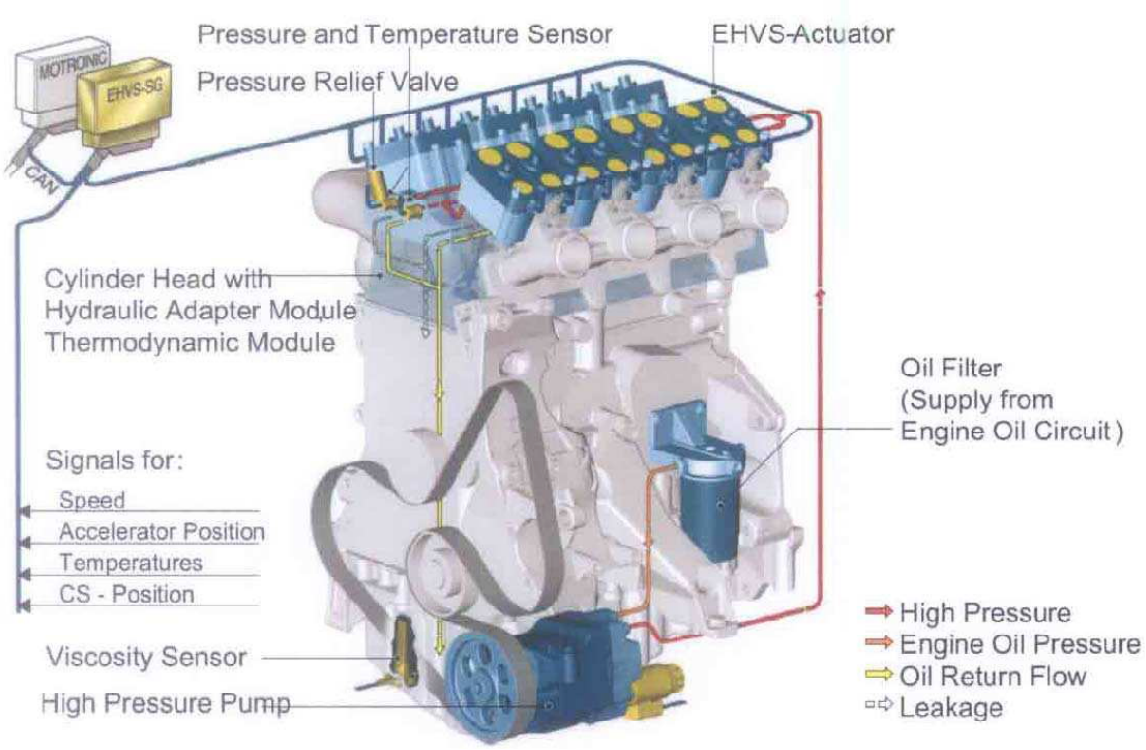

Figure 1.2: EHVS placement on a four cylinder/sixteen valve engine [7]

there are direct affects on charge motion, pumping losses and dissipation.

Last, within the EHVS two parameters can be modified in order to improve engine operation. The closing ramp of the valve lift function, the variable damping, is able to vary the closing ramp velocity independent of the hydraulic pressure. With this pumping losses, charge motion, volumetric efficiency, and intake system acoustics can be improved. Finally the hydraulic pressure of the system is the main parameter for adapting the valve lift function to speed and load. Also, this can be adjusted to reduce the parasitic losses of the valvetrain.

1.3 Alternatives to EHVS

As previously discussed, there is the mechanical solution to provide VVT and variable valve lift in engines developed by [16]. However given the improvements offered by a camless engine, there have been many alternate solutions proposed.

Other methods of VVT include valve control with solenoid actuators [26], clapper type solenoid actuators [15], pneumatics [14], electrical motors [19], piezo-electrics [3], and other hydraulic actuators [6] and [24].

There has been extensive research in the electro-mechanical valve (EMV) which is discussed in the paper by [26]. Like EHVS, with appropriate control schemes EMV offers improvements to standard internal combustion engine performance as discussed by [21]. Work has gone into modeling [5] the EMV to allow for better control. EMV has also had extensive controls work applied to the system. For instance [8] achieved sensorless control of the actuator, however there have been problems with soft seating and high voltages associated with the operation of EMV.

[13] has developed permanent magnet actuator to improve the EMV, and reduce the operating voltages. However, even with these improvements, there are many difficulties in achieving soft landings with the EMV actuator [26]. [20] address the high impact velocities via an extremum seeking method based on microphone measurements. In addition, [11] developed an iterative algorithm to achieve soft landings. [4] has created a valve control method on clapper type solenoid actuators to address soft seating with a non-linear observer. EHVS addresses the landing problems with a variable damping mechanism that increases the damping as the valve comes to a close.

1.4 Past Hydraulic Controls Work

Because of the wide range of industrial applications the past work in hydraulic system control has utilized various control techniques. For instance [9] used linear control theory and [25] utilized feedback linearization in their respective hydraulic control problems. Recently quantitative feedback theory, in [18] and [17], and backstepping design technique [28] have been used to create robust controllers. However, it is in [1] where nonlinear adaptive control is applied in the presence of parametric uncertainties. They show, experimentally, how an active nonlinear adaptive control scheme improves performance over a non-adaptive scheme. In addition [2] developed simplifications to their control scheme without too much performance loss. Also [27] utilized an adaptive robust control to overcome both parametric uncertainties and un-

certain nonlinearities in a single rod hydraulic actuator. With their adaptive robust motion control algorithm they achieved more than a order of magnitude reduction in tracking errors over a PID motion controller.

There has also been work in automotive electro-hydraulic camless valvetrains controls. In [6] creates a hydraulic system solely to achieve VVT. The hydraulic system described by [6] is limited in valve lift and has a fixed seating velocity. Therefore the main objective of the controller is synchronization of the valves to achieve optimum timing. While this system achieves the benefits of VVT, the ability of variable valve lift is lost. However, [24] creates an adaptive lift controller for an electro-hydraulic system. The resulting controller, which models the system as a variable gain linear system, experimentally proved more effective then a PID controller.

1.5 Contributions and Contents of the Thesis

Given the success of the prior nonlinear adaptive control schemes as well as parameters, such as the bulk modulus which is dependent on pressure and temperature [29], which vary during operation we create an on-line parameter identification technique for EHVS. This thesis uses a more complex hydraulic system model to develop a parameter identifier for use in future control schemes. We follow techniques found in [12] to create an exponentially convergent least squares identifier with a forgetting factor for the unknown parameters.

We first develop the theory behind the identifiers. We describe how to develop a linear parametric model through filtering and then develop the least squares and gradient identifiers. Finally we prove the stability and convergence rates of the algorithms.

After the discussion of theory, we move to the model development of the EHVS. We create a physics based model of the system and discuss its operation. In addition, we create a mathematical representation of the variable damping term.

The identifiers of the EHVS model are then explicitly developed. In order to deal with the non-linearities in the variable damping term, we create a Taylor expansion to linearize the terms. Using the structure of the model, we create two three dimensional identification problems and develop the update law.

We present the results of the simulations. We show stable operation of the system states and persistence of excitation of the signals which are important for the stability of the identifier. We show the failure of a "pure" least squares to quickly adapt, and the strong convergence properties of the least squares with forgetting factor in perfect and noisy applications.

Lastly we create a hybrid model of the EHVS to more accurately simulate behavior of the system when the valve is closed. We apply the least squares identifier, along with a switching least squares identifier and achieve similar convergence properties to the original case.

This chapter is in part an adaptation of material as it appears in J. Gray, M. Krstic, N. Chaturvedi, P. Sungbae, A. Kojic, K. Mischker "Parameter Identification for Electrohydaulic Valvetrain Systems," which was submitted to the *ASME Journal of Dynamic Systems, Measurement and Control*. The thesis author was the principle researcher and author of this paper.

2

Identifier Theory

2.1 Introduction

In this chapter we will first briefly introduce the background of the filtered linear parametric model in the general case. Secondly we introduce the unnormalized continuous-time recursive least squares algorithm with forgetting factor. After developing the algorithm, we prove polynomial convergence of the "pure" least squares and exponential convergence of the least squares with forgetting factor. Lastly we give a gradient based identifier and prove an exponential convergence rate to the true parameter. In all cases a persistence of excitation of the regressor vector is necessary to guarantee convergence.

2.2 Parametric Modeling

Following the methods in section 2.4 of [12], we start from the general transfer function description,

$$y = \frac{Z(s)}{R(s)} u \tag{2.1}$$

in which $Z(s)$ and $R(s)$ can be represented as

$$\begin{aligned} Z(s) &= b_{n-1}s^{n-1} + b_{n-2}s^{n-2} + \ldots + b_1 s + b_0 \\ R(s) &= s^n + a_{n-1}s^{n-1} + \ldots + a_1 s + a_0 \,. \end{aligned} \tag{2.2}$$

If $Z(s)$ is of degree $m < n-1$ then the coefficients $b_i = 0$ with $i = n-1, n-2, \ldots, m+1$. Taking equation (2.1) we can express it as the following nth-order differential equation

$$y^{(n)} + a_{n-1}y^{(n-1)} + \ldots + a_0 y = b_{n-1}u^{(n-1)} + b_{n-2}u^{(n-2)} + \ldots + b_0 u\,. \tag{2.3}$$

Then we collect all unknown parameters in (2.3) which can appear on both sides into the parameter vector

$$\theta = [b_{n-1}, b_{n-2}, \ldots, b_0, a_{n-1}, a_{n-2}, \ldots, a_0]^T$$

and collect the other inputs and output signals and their derivatives associated with the unknown parameters in the regressor vector

$$\begin{aligned}\phi &= \left[u^{(n-1)}, u^{(n-2)}, \ldots, u, -y^{(n-1)}, -y^{(n-2)}, \ldots, -y\right]^T \\ &= \left[\alpha_{n-1}^T(s)u, -\alpha_{n-1}^T(s)y\right]^T\end{aligned}$$

with $\alpha_i(s) \triangleq [s^i, s^{i-1}, \ldots, 1]^T$, we rewrite (2.3) in the compact form

$$y^{(n)} = \theta^T \phi\,. \tag{2.4}$$

The equation (2.4) is linear in θ, which is necessary for the designing the identifiers developed in the next section. We can estimate the unknowns of θ from measurements of $y^{(n)}$ and ϕ. However, most applications have only measurements available from the input u and the output y. Since the use of differentiation is not desirable, higher order signals should be avoided. To circumvent the need of such signals in $y^{(n)}$ and ϕ, we filter each side of (2.4) with an nth-order stable filter $\frac{1}{\Lambda(s)}$ to obtain

$$Y = \theta^T \Phi \tag{2.5}$$

with

$$\begin{aligned}Y &\triangleq \frac{1}{\Lambda(s)}y^{(n)} = \frac{s^n}{\Lambda(s)}y \\ \Phi &\triangleq \left[\frac{\alpha_{n-1}^T(s)}{\Lambda(s)}u, -\frac{\alpha_{n-1}^T(s)}{\Lambda(s)}y\right]^T\end{aligned}$$

and with

$$\Lambda(s) = s^n + \lambda_{n-1}s^{n-1} + \ldots + \lambda_0$$

being a Hurwitz polynomial in s. From this it can be seen that the scalar Y and the vector signal Φ can be generated by filtering the input u and output y with stable proper filters $\frac{s^i}{\Lambda(s)}$, where $i = 0, 1, \ldots, n$. In the event that certain parameters are known beforehand the terms in equation (2.5) change appropriately. The known values will be shifted into the scalar valued Y. For example if all the coefficients of $R(s)$ are known parameters Y is now

$$Y = \frac{s^n + a_{n-1}s^{n-1} + \ldots + a_1 s + a_0}{\Lambda(s)} y$$

and

$$\theta = [b_{n-1}, b_{n-2}, \ldots, b_0]^T$$
$$\Phi = \left[\frac{\alpha_{n-1}^T(s)}{\Lambda(s)} u\right]^T$$

From this equation setup we can create the parameter identifier for the unknown parameters in θ as described in the following sections.

2.3 Least-Squares Identifier

In this section we develop the *unnormalized continuous-time recursive least-squares algorithm with forgetting factor* [12] based on the linear parametric model (2.5) developed in Section 2.2. As an overview the least squares algorithm will attempt to estimate $\hat{\theta}(t)$ of the unknown parameter vector $\theta(t)$ by fitting the mathematical model to a sequence of observed data. It achieves this by minimizing the sum of the squared difference between observed and computed data. The forgetting factor focuses the algorithm on more recent data. To begin we consider the following cost function,

$$J\left(\hat{\theta}\right) = \frac{1}{2}\int_0^t e^{-\beta(t-\tau)}\left[Y(\tau) - \Phi^T(\tau)\,\hat{\theta}\,(t)\right]^2 d\tau + \frac{1}{2}e^{-\beta t}\left(\hat{\theta} - \hat{\theta}_0\right)^T Q_0\left(\hat{\theta} - \hat{\theta}_0\right) \quad (2.6)$$

where $Q_0 = Q_0^T > 0$, $\beta \geq 0$, and $\hat{\theta}_0 = \hat{\theta}(0)$. The design constant β acts as a forgetting factor to focus estimation on the most recent data. The effect of the old data at time $\tau < t$ is discarded exponentially when $\beta > 0$. The parameter $\hat{\theta}(t)$ should be chosen at each time t to minimize the integral square of the error on all exponentially discounted past data. Additionally there is a term to penalize the initial parameter

error. Assuming $Y, \Phi \in \mathcal{L}_\infty$, $J(\hat{\theta})$ is a convex function of $\hat{\theta}$ over $\mathcal{R}^n$ at each time t. Therefore any local minimum is also global and satisfies

$$\nabla J\left(\hat{\theta}(t)\right) = 0, \quad \forall t \geq 0$$

which when expanded is

$$\nabla J\left(\hat{\theta}(t)\right) = e^{-\beta t} Q_0 \left(\hat{\theta}(t) - \hat{\theta}_0\right) - \int_0^t e^{-\beta(t-\tau)} \Phi(\tau) \left[Y(\tau) - \Phi^T(\tau)\, \hat{\theta}\,(t)\right] d\tau = 0\,.$$

This yields the *nonrecursive least-squares* algorithm after isolating $\hat{\theta}$ as follows

$$\hat{\theta}(t) = \Gamma(t) \left[e^{-\beta t} Q_0 \hat{\theta}_0 + \int_0^t e^{-\beta(t-\tau)} \Phi(\tau) Y(\tau) d\tau\right] \tag{2.7}$$

where

$$\Gamma(t) = \left[e^{-\beta t} Q_0 + \int_0^t e^{-\beta(t-\tau)} \Phi(\tau) \Phi^T(\tau) d\tau\right]^{-1}. \tag{2.8}$$

Since $Q_0 = Q_0^T > 0$ and $\Phi\Phi^T$ is positive semidefinite, $\Gamma(t)$ exists at each time t. Calculation of the inverse can be avoided by using the identity

$$\frac{d}{dt}\Gamma\Gamma^{-1} = \dot{\Gamma}\Gamma^{-1} + \Gamma\frac{d}{dt}\Gamma^{-1} = 0\,.$$

Rearranging the above expression and substituting in equation (2.8) yields

$$\begin{aligned}
\dot{\Gamma} &= -\Gamma\left[-\beta e^{-\beta t} Q_0 - \beta \int_0^t e^{-\beta(t-\tau)} \Phi(\tau)\Phi(\tau) d\tau + \Phi\Phi\right]\Gamma \\
&= -\Gamma\left[-\beta\Gamma^{-1} + \Phi\Phi^T\right]\Gamma\,,
\end{aligned}$$

resulting in Γ satisfying the differential equation

$$\dot{\Gamma} = \beta\Gamma - \Gamma\Phi\Phi^T\Gamma, \quad \Gamma(0) = \Gamma_0 = Q_0^{-1}\,. \tag{2.9}$$

As such, we can calculate Γ as the solution to the differential equation (2.9). Next, we differentiate (2.7) with respect to time which gives

$$\begin{aligned}
\dot{\hat{\theta}} =& \Gamma\left[-\beta e^{-\beta t} Q_0 \hat{\theta}_0 - \beta \int_0^t e^{-\beta(t-\tau)} Y(\tau)\Phi(\tau) d\tau + \Phi Y\right] \\
&+ \dot{\Gamma}\left[e^{-\beta t} Q_0 \hat{\theta}_0 + \int_0^t e^{-\beta(t-\tau)} Y(\tau)\Phi(\tau) d\tau\right],
\end{aligned}$$

then substituting (2.9) for $\dot{\Gamma}$ yields

$$\dot{\hat{\theta}} = \Gamma\Phi Y - \Gamma\Phi\Phi^T\Gamma\left[e^{-\beta t}Q_0\hat{\theta}_0 + \int_0^t e^{-\beta(t-\tau)}Y(\tau)\Phi(\tau)d\tau\right]. \tag{2.10}$$

Finally, substituting equation (2.7) into (2.10) and collecting terms results in the update law

$$\dot{\hat{\theta}} = \Gamma\Phi\left(Y - \Phi^T\hat{\theta}\right), \quad \hat{\theta}(0) = \hat{\theta}_0\,. \tag{2.11}$$

Equations (2.9) and (2.11) are known as the *continuous-time recursive least-squares algorithm with forgetting factor.*

2.4 Stability of Least-Squares Algorithm

In this section we will prove the stability and convergence properties of the unnormalized least squares algorithm in two different cases. The first case is when $\beta = 0$ in equation (2.9). Setting $\beta = 0$, $\tilde{\theta} = \theta - \hat{\theta}$, and $Y = \Phi^T\theta$ we restate equations (2.11) and (2.9) as

$$\begin{aligned}\dot{\hat{\theta}} &= \Gamma\Phi\Phi^T\tilde{\theta} \\ \dot{\Gamma} &= -\Gamma\Phi\Phi^T\Gamma, \quad \Gamma(0) = \Gamma_0\end{aligned} \tag{2.12}$$

which yields the algorithm often referred to as the *"pure" least squares algorithm.* However, with the pure least squares algorithm there is a problem of covariance wind-up. Looking at the derivative of Γ^{-1} shows

$$\frac{d}{dt}\Gamma^{-1} = \Phi\Phi^T\,.$$

This implies that $\frac{d}{dt}\Gamma^{-1} \geq 0$ which implies that Γ^{-1} may grow without bound. In some cases, this can cause Γ to become small and slow estimation in some directions. However, even with this issue the algorithm guarantees parameter convergence to a constant value. That constant value is exactly θ if $\Phi \in \mathcal{L}_\infty$ and described by the following definition:

Definition 2.1 Persistence of Excitation (PE) *A piecewise continuous signal vector* $\Phi : \mathcal{R}^+ \longmapsto \mathcal{R}^n$ *is PE in* $\mathcal{R}^n$ *with a level of excitation* $\alpha_0 > 0$ *if there exist constants* α_1,$T_0 > 0$ *such that*

$$\alpha_1 I \geq \frac{1}{T_0}\int_t^{t+T_0} \Phi(\tau)\Phi^T(\tau)d\tau \geq \alpha_0 I, \quad \forall t \geq 0 \tag{2.13}$$

So while the matrix $\Phi(\tau)\Phi^T(\tau)$ is singular for every τ, equation (2.13) requires the variation of $\Phi(t)$ in time such that the integral of the matrix $\Phi(\tau)\Phi^T(\tau)$ is uniformly positive definite over any time interval $[t, t+T_0]$. Using definition (2.1) we make the following proposition:

Proposition 2.1 *The pure least-squares algorithm (2.12) guarantees that*

(i) $\Phi^T\tilde{\theta}$, $\hat{\theta}$, $\dot{\hat{\theta}}$, $\Gamma \in \mathcal{L}_\infty$.

(ii) $\Phi^T\tilde{\theta}$, $\dot{\hat{\theta}} \in \mathcal{L}_2$.

(iii) $\lim_{t\to\infty}\hat{\theta}(t) = \bar{\theta}$, *where* $\bar{\theta}$ *is a constant vector.*

(iv) *If* $\Phi \in \mathcal{L}_\infty$ *and* Φ *is PE, then* $\hat{\theta}$ *converges to* θ *as* $t \to \infty$

Proof:

From 2.12 we have that $\dot{\Gamma} \leq 0$ or $\Gamma(t) \leq \Gamma_0$. Because $\Gamma(t)$ is non-increasing and bounded from below (i.e. $\Gamma(t) = \Gamma^T(t) \geq 0, \forall t \geq 0$) it has a limit

$$\lim_{t\to\infty}\Gamma(t) = \bar{\Gamma}\,,$$

where $\bar{\Gamma} = \bar{\Gamma}^T \geq 0$ is a constant matrix. We now consider

$$\frac{d}{dt}\left(\Gamma^{-1}\tilde{\theta}\right) = -\Gamma^{-1}\dot{\Gamma}\Gamma^{-1}\tilde{\theta} + \Gamma^{-1}\dot{\tilde{\theta}}\,.$$

Substituting (2.9) for $\dot{\Gamma}$, and using $\dot{\tilde{\theta}} = -\dot{\hat{\theta}}$ the expression becomes

$$\frac{d}{dt}\left(\Gamma^{-1}\tilde{\theta}\right) = \Phi\Phi^T\tilde{\theta} - \Phi\left(Y - \Phi^T\hat{\theta}\right) = \Phi\Phi^T\tilde{\theta} - \Phi\Phi^T\tilde{\theta} = 0\,.$$

As such,

$$\Gamma^{-1}(t)\tilde{\theta}(t) = \Gamma_0^{-1}\tilde{\theta}(0)\,,$$

and multiplying both sides by Γ yields

$$\tilde{\theta}(t) = \Gamma(t)\Gamma_0^{-1}\tilde{\theta}(0)\,. \tag{2.14}$$

Taking the limit of $\tilde{\theta}$ as $t \to \infty$ results in

$$\lim_{t\to\infty} \tilde{\theta}(t) = \bar{\Gamma}\Gamma_0^{-1}\tilde{\theta}(0)\,.$$

This in turn implies that

$$\lim_{t\to\infty} \hat{\theta}(t) = \theta - \bar{\Gamma}\Gamma_0^{-1}\tilde{\theta} \triangleq \bar{\theta}\,.$$

Because $\Gamma(t) \leq \Gamma_0$ and $\tilde{\theta}(t) = \Gamma(t)\Gamma_0^{-1}\tilde{\theta}(0)$ we have $\hat{\theta}$, $\tilde{\theta} \in \mathcal{L}_\infty$, which, together with $\Phi \in \mathcal{L}_\infty$, implies that $\Phi^T\tilde{\theta} \in \mathcal{L}_\infty$. Let us now consider the Lyapunov function

$$V(\tilde{\theta}, t) = \frac{\tilde{\theta}^T\Gamma^{-1}(t)\tilde{\theta}}{2}\,.$$

Taking the time derivative of V yields

$$\dot{V} = -\tilde{\theta}^T\Phi\Phi^T\tilde{\theta} + \frac{\tilde{\theta}^T\Phi\Phi^T\tilde{\theta}}{2} = -(\Phi^T\tilde{\theta})^2 + \frac{(\Phi^T\tilde{\theta})^2}{2} = -\frac{\left(\Phi^T\tilde{\theta}\right)^2}{2} \leq 0\,,$$

which implies that $V \in \mathcal{L}_\infty$, $\Phi^T\tilde{\theta} \in \mathcal{L}_2$. From (2.12) we have

$$\left|\dot{\hat{\theta}}\right| \leq \|\Gamma\|\,|\Phi|\left|\Phi^T\tilde{\theta}\right| \tag{2.15}$$

Because Γ,Φ,$\Phi^T\tilde{\theta} \in \mathcal{L}_\infty$ and $\Phi^T\tilde{\theta} \in \mathcal{L}_2$, we have $\dot{\hat{\theta}} \in \mathcal{L}_\infty \bigcap \mathcal{L}_2$. To prove that $\tilde{\theta} \to 0$ as $t \to \infty$, we will show that $\Gamma(t) \to 0$ as $t \to \infty$ when Φ is PE. Because Γ^{-1} satisfies $\frac{d}{dt}\Gamma^{-1} = \Phi\Phi^T$, we can use the PE condition of Φ $\left(\text{i.e., } \int_t^{t+T_0} \Phi(\tau)\Phi^T(\tau)d\tau \geq \alpha_0 T_0 I\right)$, for some constant α_0, $T_0 > 0$, to show that

$$\Gamma^{-1}(t) - \Gamma^{-1}(0) = \int_0^t \Phi\Phi^T d\tau \geq n_0\alpha_0 T_0 I \geq \left(\frac{t}{T_0} - 1\right)\alpha_0 T_0 I\,, \tag{2.16}$$

where n_0 is the largest integer that satisfies $n_0 \leq \frac{t}{T_0}$ which means $n_0 \geq \frac{t}{T_0} - 1$. Therefore after rearrangement we find,

$$\Gamma^{-1}(t) \geq \Gamma^{-1}(0) + \left(\frac{t}{T_0} - 1\right)\alpha_0 T_0 I \geq \left(\frac{t}{T_0} - 1\right)\alpha_0 T_0 I\,.$$

Taking the inverse of last expression yields

$$\Gamma(t) \leq \left(\left(\frac{t}{T_0} - 1\right)\alpha_0 T_0\right)^{-1} I, \quad \forall t \geq T_0\,. \tag{2.17}$$

Since $\Gamma(t) \geq 0$ for all $t \geq 0$ and equation (2.17) goes to zero as $t \to \infty$ it follows that $\Gamma(t) \to 0$ as $t \to \infty$. Therefore, $\tilde{\theta}(t) = \Gamma(t)\Gamma_0^{-1}\tilde{\theta} \to 0$ as $t \to \infty$. However, only a polynomial decay rate is guaranteed for the pure least squares algorithm with the presence of PE. ■

In the second case, having $\beta > 0$, the problem of $\Gamma(t)$ becoming arbitrarily small in a direction no longer exists. With $\beta > 0$, $\Gamma(t)$ appears to be able to grow without bound since $\dot{\Gamma}$ may satisfy $\dot{\Gamma} > 0$ because $\beta\Gamma > 0$ and $\Gamma\Phi\Phi^T\Gamma$ is only positive semidefinite. One solution to this issue is to modify the algorithm by placing an upper bound on Γ. However, such modifications to the algorithm are not necessary when $\Phi \in \mathcal{L}_\infty$ and Φ is PE. The persistence of excitation property of Φ guarantees that over an interval of time the integral of $-\Gamma\Phi\Phi^T\Gamma$ is a negative definite matrix that counteracts the positive definite effect of $\beta\Gamma$.

Proposition 2.2 *If $\Phi(t)$ is uniformly bounded and persistently exciting, i.e., there exist constants $\alpha_0 > 0$ and T_0 such that*

$$\frac{1}{T_0}\int_t^{t+T_0} \Phi(\tau)\Phi^T(\tau)d\tau \geq \alpha_0 I, \qquad \forall t \geq 0, \tag{2.18}$$

then for all $\hat{\theta}(0) \in \mathbb{R}^m$, the following holds:

$$\left|\widetilde{\theta}(t)\right|^2 \leq M\left|\widetilde{\theta}(0)\right|^2 \mathrm{e}^{-\beta t} \tag{2.19}$$

where

$$M = \frac{\dfrac{1}{\lambda_{\min}(\Gamma_0)} + \dfrac{\sup_{t\geq 0}\lambda_{\max}\left\{\Phi(t)\Phi(t)^T\right\}}{\beta}}{\min\left\{\alpha_0 T_0, \frac{1}{\lambda_{\max}(\Gamma_0)}\right\} e^{-\beta T_0}}. \tag{2.20}$$

Proof: Taking the inverse of (2.9) we have

$$\dot{\Gamma}^{-1} = -\beta\Gamma^{-1} + \Phi\Phi^T \tag{2.21}$$

with initial condition

$$\Gamma_0^{-1} = \Gamma_0^{-T}, \tag{2.22}$$

which yields

$$\Gamma^{-1}(t) = \mathrm{e}^{-\beta t}\Gamma_0^{-1} + \int_0^t \mathrm{e}^{-\beta(t-\tau)}\Phi(\tau)\Phi^T(\tau)d\tau.$$

Using the condition that $\Phi(t)$ is persistently exciting we can show that for all $t \geq T_0$

$$\begin{aligned}\Gamma^{-1}(t) \geq & \int_0^t \mathrm{e}^{-\beta(t-\tau)}\Phi(\tau)\Phi^T(\tau)d\tau \\ = & \int_{t-T_0}^t \mathrm{e}^{-\beta(t-\tau)}\Phi(\tau)\Phi^T(\tau)d\tau \\ & + \int_0^{t-T_0} \mathrm{e}^{-\beta(t-\tau)}\Phi(\tau)\Phi^T(\tau)d\tau \\ \geq & \mathrm{e}^{-\beta T_0}\alpha_0 T_0 I\,. \end{aligned} \tag{2.23}$$

For $t \leq T_0$, we have

$$\begin{aligned}\Gamma^{-1}(t) \geq & \,\mathrm{e}^{-\beta t}\Gamma_0^{-1} \geq \mathrm{e}^{-\beta T_0}\Gamma_0^{-1} \\ & \geq \frac{1}{\lambda_{\max}(\Gamma_0)}\mathrm{e}^{-\beta T_0} I\,. \end{aligned} \tag{2.24}$$

Conditions (2.23) and (2.24) imply that

$$\Gamma^{-1}(t) \geq \gamma_1 I \tag{2.25}$$

for all $t \geq 0$, with

$$\gamma_1 = \min\left\{\alpha_0 T_0, \frac{1}{\lambda_{\max}\left(\Gamma_0\right)}\right\}\mathrm{e}^{-\beta T_0}\,. \tag{2.26}$$

For the upper limit we can use the boundedness of Φ and establish

$$\begin{aligned}\Gamma^{-1}(t) & \leq \Gamma_0^{-1} + \sup_{t\geq 0}\lambda_{\max}\left\{\Phi(t)\Phi(t)^T\right\}\int_0^t \mathrm{e}^{-\beta(t-\tau)}d\tau I \\ & \leq \gamma_2 I \end{aligned} \tag{2.27}$$

where

$$\gamma_2 = \frac{1}{\lambda_{\min}(\Gamma_0)} + \frac{\sup_{t\geq 0}\lambda_{\max}\left\{\Phi(t)\Phi(t)^T\right\}}{\beta}\,. \tag{2.28}$$

Combining (2.25) and (2.27) we get

$$\gamma_1 I \leq \Gamma^{-1}(t) \leq \gamma_2 I \tag{2.29}$$

with $\gamma_1 > 0$,$\gamma_2 > 0$ and therefore,

$$\gamma_2^{-1} I \leq \Gamma(t) \leq \gamma_1^{-1} I\,.$$

This guarantees $\Gamma, \Gamma^{-1} \in \mathcal{L}_\infty$.

With $\dot{\tilde{\theta}} = -\dot{\hat{\theta}}$ and $Y - \Phi^T\hat{\theta} = \Phi^T\tilde{\theta}$ we substitute into (2.11) to recieve

$$\dot{\tilde{\theta}} = -\Gamma\Phi\Phi^T\tilde{\theta}\,. \tag{2.30}$$

Now we proceed with the following Lyapunov function

$$V = \tilde{\theta}^T\Gamma^{-1}\tilde{\theta}\,. \tag{2.31}$$

Taking the derivative of (2.31) in time yields

$$\dot{V} = 2\dot{\tilde{\theta}}^T\Gamma^{-1}\tilde{\theta} + \tilde{\theta}^T\dot{\Gamma}^{-1}\tilde{\theta}\,.$$

Substituting (2.21) and (2.30) into the previous equation results in

$$\begin{aligned}\dot{V} &= -2\tilde{\theta}^T\Phi\Phi^T\Gamma\Gamma^{-1}\tilde{\theta} + \tilde{\theta}^T\left(-\beta\Gamma^{-1} + \Phi\Phi^T\right)\tilde{\theta} \\ &= -\tilde{\theta}^T\Phi\Phi^T\tilde{\theta} - \tilde{\theta}^T\beta\Gamma^{-1}\tilde{\theta} \leq 0\,.\end{aligned} \tag{2.32}$$

Since $-\tilde{\theta}^T\Phi\Phi^T\tilde{\theta}$ is negative definite and β is a positive scalar value we bound (2.32) by

$$\dot{V} \leq -\beta V \tag{2.33}$$

which could be rewritten as

$$V(t) \leq V_0\mathrm{e}^{-\beta t}, \quad \forall t \geq 0\,. \tag{2.34}$$

Now we take the original Lyapunov equation (2.31) and combine it with the results of (2.29) to bound $V(t)$ as follows

$$\gamma_1\left|\tilde{\theta}(t)\right|^2 \leq V(t) \leq \gamma_2\left|\tilde{\theta}(t)\right|^2\,. \tag{2.35}$$

Knowing that the upper bound of $V(t)$ can be described with (2.34), from (2.35) we get

$$\left|\tilde{\theta}(t)\right|^2 \leq \frac{1}{\gamma_1}V(t) \leq \frac{1}{\gamma_1}V_0\mathrm{e}^{-\beta t}\,. \tag{2.36}$$

Finally, substituting $\gamma_2\left|\tilde{\theta}(0)\right|^2$ as the maximum value of V_0 we get the result

$$\left|\tilde{\theta}(t)\right|^2 \leq \frac{\gamma_2}{\gamma_1}\left|\tilde{\theta}(0)\right|^2\mathrm{e}^{-\beta t}\,.$$

■

2.5 Gradient Algorithm

In this section we develop the gradient algorithm found in Section 4.3.5 of [12] which will also be based on the linear parametric model developed in Section 2.2. While the least squares with forgetting factor algorithm is an exponentially convergent identifier, the calculation of the gain matrix Γ in addition to updating the estimate $\hat{\theta}$ can be computationally intensive. The gradient method has a static gain matrix thus eliminating the need for the calculations of Γ. The gradient algorithm relies on minimizing an instantaneous cost function. It updates the estimate $\hat{\theta}$ based only on the current error of the system as opposed to the sum of the squared differences. We now consider the simpler cost function,

$$J(\hat{\theta}) = (Y - \Phi^T\hat{\theta})^2 \,. \tag{2.37}$$

That we would like to minimize with respect to the estimate $\hat{\theta}$. Because $J(\hat{\theta})$ is convex over the $\hat{\theta}$ at each time t the minimization is well posed. We want to choose $\hat{\theta}$ such that it minimizes J. The trajectory of $\hat{\theta}(t)$ is therefore generated by

$$\dot{\hat{\theta}} = -\Gamma\nabla J(\hat{\theta}) \tag{2.38}$$

where $\Gamma = \Gamma^T > 0$ is now a static scaling matrix often referred to as the adaptive gain. From (2.37) we get

$$\nabla J(\hat{\theta}) = -\Phi^T\left(Y - \Phi^T\hat{\theta}\right) \,. \tag{2.39}$$

Which, after substituting into (2.38) yields the update law

$$\dot{\hat{\theta}} = \Gamma\Phi^T\left(Y - \Phi^T\hat{\theta}\right) \,. \tag{2.40}$$

Equation (2.40) is known as the gradient algorithm.

2.6 Stability of the Gradient Algorithm

In this section we will prove the stability and convergence properties of the gradient algorithm. From (2.39) we have that the minimum of $J(\hat{\theta})$ occurs when $Y - \Phi^T\hat{\theta} = 0$ which implies $\dot{\hat{\theta}} = 0$ thus ending adaptation of the identifier. It can be shown, using a Lyapunov type of analysis, that $\hat{\theta}$ will converge to the actual value θ exponentially fast in time.

Proposition 2.3 *The gradient adaptive law (2.40) guarantees that*

(i) $Y - \Phi^T\hat{\theta}$, $\hat{\theta}$, $\dot{\hat{\theta}} \in \mathcal{L}_\infty$.

(ii) $Y - \Phi^T\hat{\theta}$, $\dot{\hat{\theta}} \in \mathcal{L}_2$.

independent of the boundedness of the regressor vector Φ *and*

(iii) *If* $\Phi \in \mathcal{L}_\infty$ *and* Φ *is PE, then* $\hat{\theta}$ *converges to* θ

Proof: Taking $\dot{\tilde{\theta}} = -\dot{\hat{\theta}}$ and substituting into equation (2.40) we get

$$\dot{\tilde{\theta}} = -\Gamma\Phi\Phi^T\tilde{\theta}\,. \tag{2.41}$$

Like before we chose the Lyapunov function

$$V(\tilde{\theta}) = \frac{\tilde{\theta}^T\Gamma^{-1}\tilde{\theta}}{2}\,.$$

Taking the derivative of V in time yields

$$\dot{V} = -\tilde{\theta}^T\Phi\Phi^T\tilde{\theta} = -\left(\Phi^T\tilde{\theta}\right)^2 \leq 0\,. \tag{2.42}$$

Therefore V,$\tilde{\theta} \in \mathcal{L}_\infty$ which implies that $\left(Y - \Phi^T\hat{\theta}\right) \in \mathcal{L}_\infty$. In addition, from the properties of V and $\dot{V}$ we find that $\tilde{\theta}$, $\left(Y - \Phi^T\hat{\theta}\right) \in \mathcal{L}_2$. From (2.41) we have

$$\left|\dot{\tilde{\theta}}\right| = \left|\dot{\hat{\theta}}\right| \leq \|\Gamma\| \left|\Phi\Phi^T\right| \left|\tilde{\theta}\right| \tag{2.43}$$

which, along with $\left|\Phi^T\right| \in \mathcal{L}_\infty$ and $\tilde{\theta} \in \mathcal{L}_2 \bigcap \mathcal{L}_\infty$ implies that $\dot{\hat{\theta}} \in \mathcal{L}_2 \bigcap \mathcal{L}_\infty$.

To prove exponential stability we expand equation (2.42) into

$$V\left(t+T\right) = V(t) - \int_t^{t+T} \left(\Phi^T(\tau)\tilde{\theta}(\tau)\right)^2 d\tau \tag{2.44}$$

for any t, $T > 0$. We express $\Phi^T(\tau)\tilde{\theta}(\tau)$ as,

$$\Phi^T(\tau)\tilde{\theta}(\tau) = \Phi^T(\tau)\tilde{\theta}(t) + \Phi^T(\tau)\left(\tilde{\theta}(\tau) - \tilde{\theta}(t)\right)$$

and noting the inequality $(x+y)^2 \geq \frac{1}{2}x^2 - y^2$ it follows that

$$\begin{aligned}\int_t^{t+T} \left(\Phi^T(\tau)\tilde{\theta}(\tau)\right)^2 d\tau \geq & \frac{1}{2}\int_t^{t+T} \left(\Phi^T(\tau)\tilde{\theta}(t)\right)^2 d\tau \\ & - \int_t^{t+T} \left(\Phi^T(\tau)\left(\tilde{\theta}(\tau) - \tilde{\theta}(t)\right)\right)^2 d\tau\,.\end{aligned} \tag{2.45}$$

Using the PE property of Φ, i.e.,

$$\int_t^{t+T_0} \Phi^T(\tau)\Phi(\tau)d\tau \geq \alpha_0 T_0 I$$

for some T_0 and $\alpha_0 > 0$, we have

$$\int_t^{t+T_0} \left(\Phi^T(\tau)\tilde{\theta}(t)\right)^2 d\tau \geq \alpha_0 T_0 \tilde{\theta}^T(t)\tilde{\theta}(t) \geq 2\alpha_0 T_0 \lambda_{\min}(\Gamma) V(t). \tag{2.46}$$

For the second part of (2.45) we can write

$$\tilde{\theta}(\tau) - \tilde{\theta}(t) = \int_t^\tau \dot{\tilde{\theta}}(\sigma)d\sigma = -\int_t^\tau \Gamma\Phi(\sigma)\Phi(\sigma)^T\tilde{\theta}(\sigma)d\sigma$$

which leads to

$$\Phi^T(\tau)\left(\tilde{\theta}(\tau) - \tilde{\theta}(t)\right) = \int_t^\tau \Phi^T(\tau)\Gamma\Phi(\sigma)\Phi(\sigma)^T\tilde{\theta}(\sigma)d\sigma. \tag{2.47}$$

Using the Schwartz inequality and (2.47) we find

$$\begin{aligned}
&\int_t^{t+T} \left(\Phi^T(\tau)\left(\tilde{\theta}(\tau) - \tilde{\theta}(t)\right)\right)^2 d\tau \\
\leq &\int_t^{t+T} \left(\int_t^\tau \left(\Phi^T(\tau)\Gamma\Phi(\sigma)\right)^2 d\sigma \int_t^\tau \left(\Phi(\sigma)^T\tilde{\theta}(\sigma)\right)^2 d\sigma\right) d\tau \\
\leq &\eta^4\lambda_{\max}^2(\Gamma)\int_t^{t+T}(\tau - t)\int_t^\tau \left(\Phi(\sigma)^T\tilde{\theta}(\sigma)\right)^2 d\sigma d\tau
\end{aligned}$$

where $\eta = \sup_{\tau\geq 0}|\Phi(\tau)|$. We then change the sequence of integration to receive

$$\begin{aligned}
&\int_t^{t+T} \left(\Phi^T(\tau)\left(\tilde{\theta}(\tau) - \tilde{\theta}(t)\right)\right)^2 d\tau \\
\leq &\eta^4\lambda_{\max}^2(\Gamma)\int_t^{t+T}\left(\Phi^T(\sigma)\tilde{\theta}(\sigma)\right)^2\int_\sigma^{t+T}(\tau - t)\,d\tau d\sigma \\
\leq &\eta^4\lambda_{\max}^2(\Gamma)\int_t^{t+T}\left(\Phi^T(\sigma)\tilde{\theta}(\sigma)\right)^2\left[\frac{T^2 - (\sigma - t)^2}{2}\right]d\sigma \\
\leq &\frac{\eta^4\lambda_{\max}^2(\Gamma)T^2}{2}\int_t^{t+T}\left(\Phi^T(\sigma)\tilde{\theta}(\sigma)\right)^2 d\sigma.
\end{aligned} \tag{2.48}$$

Using (2.46) and (2.48) in (2.45) with $T = T_0$ we get

$$\int_t^{t+T_0} \left(\Phi^T(\tau)\tilde{\theta}(\tau)\right)^2 d\tau \geq \alpha_0 T_0 \lambda_{\min}^2(\Gamma)V(t) - \frac{\eta^4 T_0^2 \lambda_{\max}^2(\Gamma)}{2}\int_t^{t+T_0}\left(\Phi^T(\sigma)\tilde{\theta}(\sigma)\right)^2 d\sigma$$

which after rearrangement yields

$$\begin{aligned}
\int_t^{t+T_0} \left(\Phi^T(\tau)\tilde{\theta}(\tau)\right)^2 d\tau &\geq \frac{\alpha_0 T_0 \lambda_{\min}^2(\Gamma)}{1 + \frac{\eta^4 T_0^2 \lambda_{\max}^2(\Gamma)}{2}} V(t) \\
&\geq \kappa_1 V(t)
\end{aligned} \tag{2.49}$$

where $\kappa_1 = \frac{2\alpha_0 T_0 \lambda_{\min}(\Gamma)}{2+\eta^4 T_0^2 \lambda^2_{\max}(\Gamma)}$. Using (2.49) in (2.44) with $T = T_0$, it follows that

$$V(t+T_0) \leq V(t) - \kappa_1 V(t) = \kappa V(t) \tag{2.50}$$

where $\kappa = 1 - \kappa_1$. Since $\kappa_1 > 0$ and $V(t+T_0) \geq 0$, we have $0 < \kappa < 1$. Since (2.50) holds for all $t \geq 0$ we can take $t = (n-1)\,T_0$ and use (2.50) successively to receive

$$V(t) \leq V(nT_0) \leq \kappa^n V(0)\,, \quad \forall t \geq nT_0,\, n = 0, 1, \ldots\,.$$

Therefore, $V(t) \to 0$ as $t \to \infty$ exponentially fast implying that $\tilde{\theta}(t) \to 0$ as $t \to \infty$ exponentially fast. ■

With the development of the theory behind the identifiers and proof of their stability, we now move towards modeling the actual EHV System.

This chapter is in part an adaptation of material as it appears in J. Gray, M. Krstic, N. Chaturvedi, P. Sungbae, A. Kojic, K. Mischker "Parameter Identification for Electrohydaulic Valvetrain Systems," which was submitted to the *ASME Journal of Dynamic Systems, Measurement and Control*. The thesis author was the principle researcher and author of this paper.

3

Model Development of EHVS

3.1 Introduction

In this chapter we introduce the model of the EHV System. We discuss the system operation, parameter assumptions and introduce a model for the variable damping nonlinearity. The model contains an unknown parameter that appears non-linearly, which creates a problem for the linear parametric model. Therefore, we develop a Taylor expansion of the variable damping to facilitate creating the linear parametric model.

3.2 Model of EHV System

Consider the model of the EHVS system based on the Figure 3.1 given by two differential equations,

$$M_t\ddot{x}_p = A_{p_1}P_1 - A_{p_2}P_s - F_o - B\dot{x}_p - RB \tag{3.1}$$

$$Q_1 - Q_2 = \dot{V}_1 + \frac{V_1}{\beta_e}\dot{P}_1 \tag{3.2}$$

and three algebraic equations,

$$V_1 = V_{o_1} + A_{p_1}x_p \tag{3.3}$$

$$Q_1 = C_{d1}w_1x_{v1}\mathrm{sgn}\left(P_s - P_1\right)\sqrt{\frac{2\left|P_s - P_1\right|}{\rho}} \tag{3.4}$$

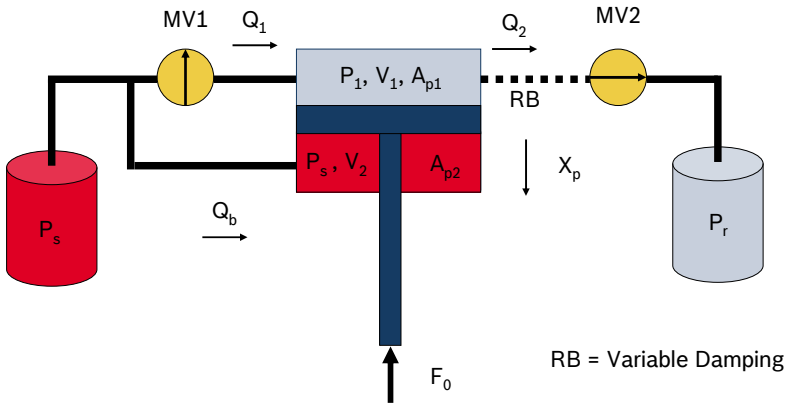

Figure 3.1: Schematic of the EHVS

$$Q_2 = C_{d2} w_2 x_{v2} \text{sgn}\left(P_1 - P_r\right) \sqrt{\frac{2\left|P_1 - P_r\right|}{\rho}}, \tag{3.5}$$

where the model variables are defined in the list of symbols. The system has three states, P_1, x_p, $\dot{x}_p$, two inputs which are available to the designer, x_{v_1}, x_{v_2}, three inputs that are not available to the designer, P_s, P_r, F_0, three variables that algebraically depend on the states V_1, Q_1, Q_2 and the remaining are system parameters. Of these equations it is assumed that only the parameters V_{0_1}, M_t, A_{p_1}, and A_{p_2} are known precisely.

This model is physics based. Equation (3.1) is the kinematic equation for motion in the engine valve. The other differential equation (3.2) relates the fluid flow into the top chamber and the effects on displacement and pressure. The three algebraic equations are conversions for equation (3.2). Equation (3.3) is a position to volume conversion, while equations (3.4) and (3.5) govern the flow from x_{v_1} and x_{v_2} respectively. The solenoid valves have dynamics, which [22] have done work in modeling, however in this model those input dynamics are neglected. In our model the solenoid valves x_{v_1} and x_{v_2} are considered to be the discrete inputs of the system. Solenoid valve x_{v_1} is normally closed and the other solenoid valve is normally open. This leaves the valve in fail safe "engine valve closed" position since P_1 is exposed to P_r.

Figure 3.2 displays the operation of the EHV System through the major solenoid valve events. In order to create movement in the system, valve x_{v_2} closes while x_{v_1} opens letting high pressure (P_s) into the top chamber. The difference in surface area

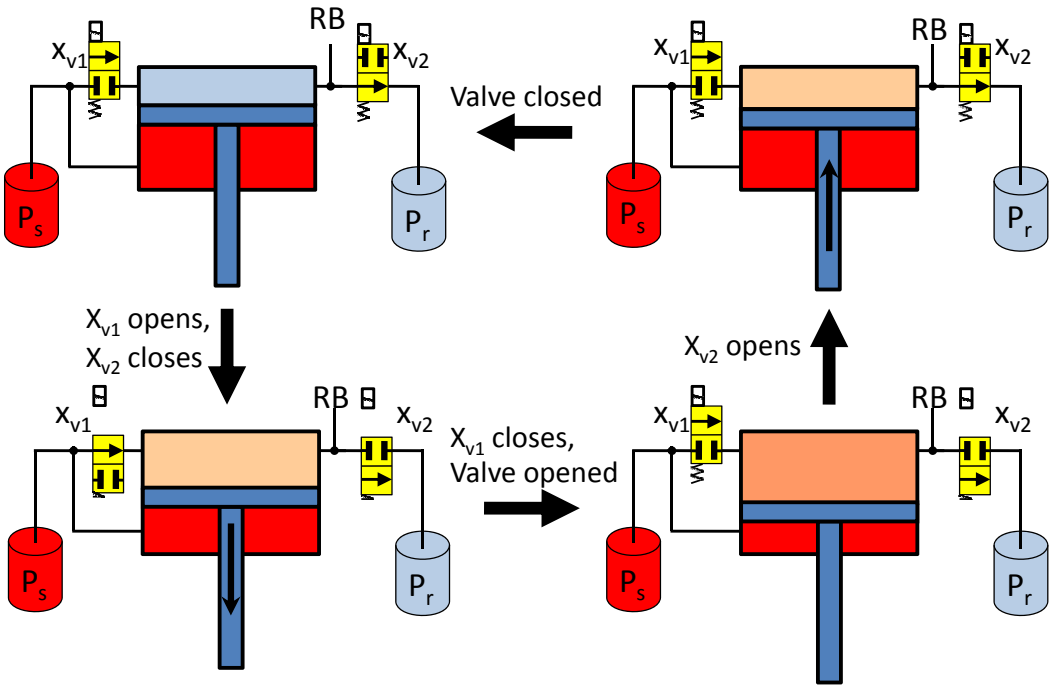

Figure 3.2: Operation cycle of the EHVS

($A_{p1} > A_{p2}$) creates downward movement in the system. After reaching the desired lift x_{v1} closes. With both valves closed, the lift settles to a steady state. To close the valve x_{v_2} opens exposing the top chamber to the reservoir pressure (P_r) and forcing upward movement. Since the valve hits a mechanical stop when it closes, x_{v_2} is left open until the beginning of the next cycle. There is an inclusion of variable damping term RB which is responsible for the soft seating of the valve. This term will be introduced in Section 3.3.

It may appear that there are seven uncertain physical parameters, β_e, B, C_{d_1}, C_{d_2}, w_1, w_2, ρ. However, only four can be identified independently from the measured signals. The identifiable terms are the compressibility coefficient β_e, the damping of the valve piston B, and the "combination" coefficients $C_{d_1} w_1 \sqrt{\frac{2}{\rho}}$ and $C_{d_2} w_2 \sqrt{\frac{2}{\rho}}$ which contain the solenoid valve discharge coefficients, area gradients of the solenoid valve ports, and the density of the hydraulic fluid.

3.3 Model of Variable Damping Nonlinearity

Equation (3.1) contains the variable damping term RB. Since the effect of the variable damping is a swift increase of damping as the valve comes to close, we take the following representation

$$RB(x_p, \dot{x}_p) = \frac{\dot{x}_p - |\dot{x}_p|}{2} \frac{D}{D_b + x_p^{2k}} \,. \tag{3.6}$$

With this model the nonlinear force acts as damping, as it is velocity dependent. In addition the damping value is a function of position. Looking at figure 3.3 the gain moves from a zero value when away from the origin to a large final value as the valve comes to a close creating the desired affect.

The velocity term $\frac{\dot{x}_p - |\dot{x}_p|}{2}$ ensures that the variable damping force is only active during the closing of the valve. The remainder of the terms (D, D_b, and k) offer flexibility in the approximation of variable damping. Figure 3.3 shows the effects of varying D, D_b, and k. Increasing D_b increases the distance from zero that variable damping goes into effect. The maximum gain approaches the ratio of $\frac{D}{D_b}$. Finally, a larger k creates a more step-like response.

3.4 Taylor Expansion of Variable Damping

With these terms equation (3.6) gives great flexibility in the modeling of RB. However, since the unknown parameter D_b appears non-linearly, creating a linear parametric model for estimation of D_b poses a problem. To create a model of RB that is linear in D_b, we take a Taylor expansion of RB about D_b at the estimate $\widehat{D}_b$, which yields

$$\begin{aligned} RB &\approx \frac{\dot{x}_p - |\dot{x}_p|}{2} D \left(\frac{1}{\widehat{D}_b + x_p^{2k}} + \frac{-D_b + \widehat{D}_b}{\left(\widehat{D}_b + x_p^{2k}\right)^2} \right) \\ &\approx \frac{\dot{x}_p - |\dot{x}_p|}{2} D \left(\frac{2\widehat{D}_b + x_p^{2k} - D_b}{\left(\widehat{D}_b + x_p^{2k}\right)^2} \right) \\ &\approx \frac{\dot{x}_p - |\dot{x}_p|}{2} D \left(\frac{2\widehat{D}_b + x_p^{2k}}{\left(\widehat{D}_b + x_p^{2k}\right)^2} - \frac{D_b}{\left(\widehat{D}_b + x_p^{2k}\right)^2} \right) . \end{aligned} \tag{3.7}$$

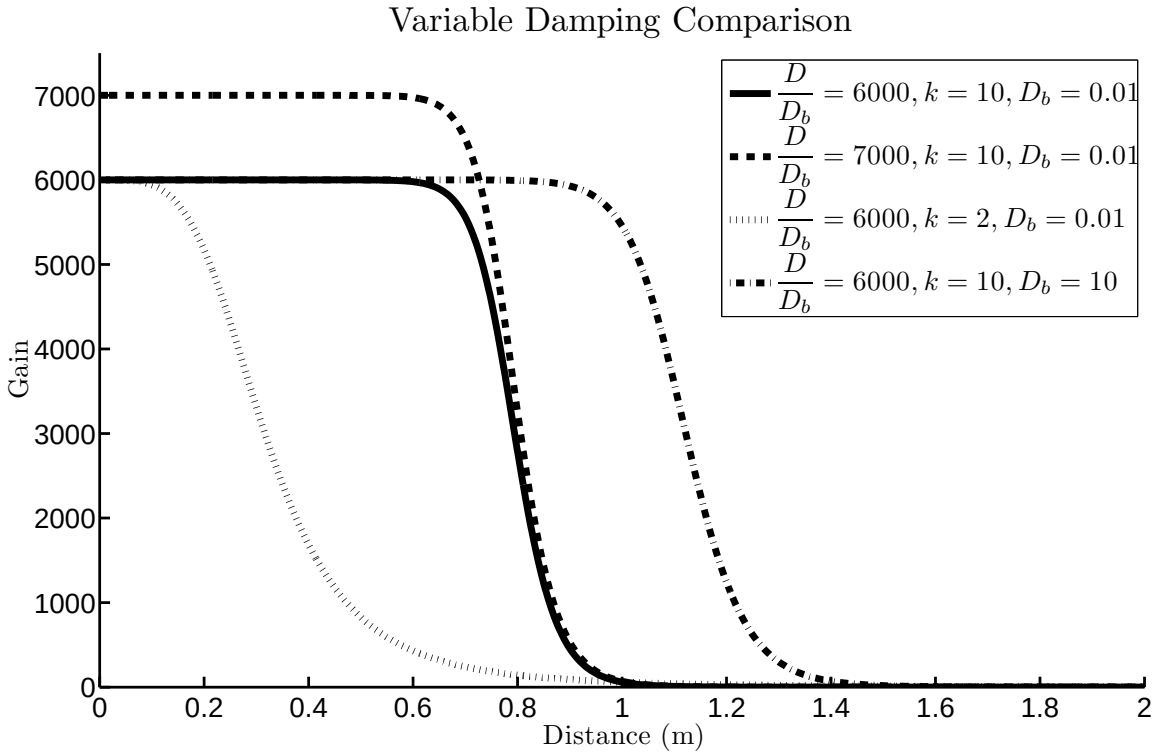

Figure 3.3: Dependence of $\frac{D}{\left(D_b + x_p^{2k}\right)}$ on D,D_b, k, and x_p.

The system is now linear in the unknown term D_b, noting that $\widehat{D_b}$ is an estimate of that parameter. Substituting equation (3.7) into equation (3.1) yields

$$\begin{aligned} M_t \ddot{x}_p =& A_{p_1} P_1 - A_{p_2} P_s - F_o - B\dot{x}_p \\ & - \frac{\dot{x}_p - |\dot{x}_p|}{2} \left[D \left(\frac{2\widehat{D_b} + x_p^{2k}}{\left(\widehat{D_b} + x_p^{2k}\right)^2} - \frac{D_b}{\left(\widehat{D_b} + x_p^{2k}\right)^2} \right) \right]. \end{aligned} \tag{3.8}$$

So now for estimation we have the unknown terms B, D, and DD_b in the piston subsystem. We use (3.8) in the parametric model for our identifier design in Chapter 2 since D_b is unknown. However, for our simulation tests we use the nonlinearly parametrized model (3.1) and (3.6) to create the soft landing of the system.

This chapter is in part an adaptation of material as it appears in J. Gray, M. Krstic, N. Chaturvedi, P. Sungbae, A. Kojic, K. Mischker "Parameter Identification for Electrohydaulic Valvetrain Systems," which was submitted to the *ASME Journal of Dynamic Systems, Measurement and Control*. The thesis author was the principle

researcher and author of this paper.

4

Identifier Development

4.1 Introduction

In this chapter we apply techniques developed in Chapter 2 to the EHV System to develop an identifier for the unknown parameters. We use the two differential equations of the system and create two identifiers for the six unknown parameters. We filter each differential equation and create two linear parametric models. We use the parametric models to define the parameter vectors θ, regressor vectors Φ, and the quantities Y for each differential equation. We then apply the terms to create the least-squares and gradient identifiers for the EHV System. Therefore we have two three dimensional identifiers for each algorithm used.

4.2 Parametric Model

The system's two differential equations which we use for identification, (3.2) and (3.8), are linear in the parameters β_e, B, D, D_b, $C_{d_1} w_1 \sqrt{\frac{2}{\rho}}$ and $C_{d_2} w_2 \sqrt{\frac{2}{\rho}}$. However (3.2) and (3.8) involve the derivative signals $\ddot{x}_p$, $\dot{x}_p$, $\dot{P}_1$, and $\dot{V}_1$ which are noisy. Unfortunately, $\dot{x}_p$ appears nonlinearly (and non-smoothly) in equation (3.8) and therefore must be treated as measurable in the parametric model. Filtering (3.2) and (3.8) with a stable first order low-pass filter of the form $\frac{1}{s+\lambda}$ creates a suitable parametric model for identification.

After filtering (3.8) we get the parametric model

$$\begin{aligned} M_t\left(\frac{\lambda}{s+\lambda}\dot{x}_p-\dot{x}_p\right)+\frac{1}{s+\lambda}\left(A_{p_1}P_1-A_{p_2}P_s\right)= \\ B\left(\frac{\lambda}{s+\lambda}x_p-x_p\right)+\frac{1}{s+\lambda}F_o \\ +D\left(\frac{1}{s+\lambda}\right)\left[\frac{\left(\dot{x}_p-|\dot{x}_p|\right)\left(\hat{D}_b+x_p^{2k}\right)}{2\left(\hat{D}_b+x_p^{2k}\right)^2}\right] \\ -DD_b\left(\frac{1}{s+\lambda}\right)\frac{\dot{x}_p-|\dot{x}_p|}{2\left(\hat{D}_b+x_p^{2k}\right)^2}\,. \end{aligned} \tag{4.1}$$

In the absence of any information on F_0, we treat $\frac{1}{s+\lambda}F_o$ as stochastic noise, otherwise it can be moved to the left as a known signal. Aside from B, D, and D_b all the signals in the model (4.1) are available and linear in the unknown parameters.

Conversion of the pressure flow equation, (3.2), into a linear parametric model requires us to first rewrite it as

$$\begin{aligned} \frac{d}{dt}P_1+\beta_e\frac{d}{dt}\ln V_1= \\ \beta_e C_{d1}w_1\sqrt{\frac{2}{\rho}}x_{v1}\mathrm{sgn}\left(P_s-P_1\right)\frac{\sqrt{|P_s-P_1|}}{V_1} \\ -\beta_e C_{d2}w_2\sqrt{\frac{2}{\rho}}x_{v2}\mathrm{sgn}\left(P_1-P_r\right)\frac{\sqrt{|P_1-P_r|}}{V_1}\,. \end{aligned} \tag{4.2}$$

Note that the signals P_1, V_1, P_s, P_r, x_{v_1}, and x_{v_2} are available (either measured, or available as control inputs). Therefore the model (4.2) is linear in the unknown parameters β_e, $\beta_e C_{d_1}w_1\sqrt{\frac{2}{\rho}}$, and $\beta_e C_{d_2}w_2\sqrt{\frac{2}{\rho}}$ but again requires some filtering due to the unavailability of the time derivatives of P_1 and $\ln V_1$. Applying the stable low-pass filter $\frac{1}{s+\lambda}$ to (4.2), we create the parametric model

$$\begin{aligned} P_1-\frac{\lambda}{s+\lambda}P_1=\beta_e\left(\frac{\lambda}{s+\lambda}\ln V_1-\ln V_1\right) \\ +\beta_e C_{d1}w_1\sqrt{\frac{2}{\rho}}\left(\frac{1}{s+\lambda}\left[x_{v1}\mathrm{sgn}\left(P_s-P_1\right)\frac{\sqrt{|P_s-P_1|}}{V_1}\right]\right) \\ -\beta_e C_{d2}w_2\sqrt{\frac{2}{\rho}}\left(\frac{1}{s+\lambda}\left[x_{v2}\mathrm{sgn}\left(P_1-P_r\right)\frac{\sqrt{|P_1-P_r|}}{V_1}\right]\right) \end{aligned} \tag{4.3}$$

4.3 Identifier Design

The parameter identification problem is separated into two three-dimensional identification problems, (4.1) from which we estimate B, D, and DD_b, and (4.3) from which we estimate β_e, $\beta_e C_{d_1} w_1 \sqrt{\frac{2}{\rho}}$, and $\beta_e C_{d_2} w_2 \sqrt{\frac{2}{\rho}}$.

Both problems involve vector parameterizations. First we introduce the parameter vectors

$$\theta_1 = \begin{bmatrix} \theta_{11} \\ \theta_{12} \\ \theta_{13} \end{bmatrix} = \begin{bmatrix} B \\ D \\ DD_b \end{bmatrix} \tag{4.4}$$

and

$$\theta_2 = \begin{bmatrix} \theta_{21} \\ \theta_{22} \\ \theta_{23} \end{bmatrix} = \begin{bmatrix} \beta_e \\ \beta_e C_{d_1} w_1 \sqrt{\frac{2}{\rho}} \\ \beta_e C_{d_2} w_2 \sqrt{\frac{2}{\rho}} \end{bmatrix} . \tag{4.5}$$

The regressor vectors Φ_1 and Φ_2 are defined as

$$\Phi_1 = \begin{bmatrix} \frac{\lambda}{s+\lambda} x_p - x_p \\ \left(\frac{1}{s+\lambda}\right)\left(\frac{\dot{x}_p - |\dot{x}_p|}{2}\right)\left[\frac{2\widehat{D_b} + x_p^{2k}}{\left(\hat{D}_b + x_p^{2k}\right)^2}\right] \\ -\left(\frac{1}{s+\lambda}\right)\left(\frac{\dot{x}_p - |\dot{x}_p|}{2}\right)\frac{1}{\left(\hat{D}_b + x_p^{2k}\right)^2} \end{bmatrix} \tag{4.6}$$

and

$$\Phi_2 = \begin{bmatrix} \frac{\lambda}{s+\lambda} \ln V_1 - \ln V_1 \\ \frac{1}{s+\lambda}\left[x_{v1} \mathrm{sgn}\left(P_s - P_1\right) \frac{\sqrt{|P_s - P_1|}}{V_1}\right] \\ \frac{1}{s+\lambda}\left[x_{v2} \mathrm{sgn}\left(P_1 - P_r\right) \frac{\sqrt{|P_1 - P_r|}}{V_1}\right] \end{bmatrix} . \tag{4.7}$$

Combining the regressor and the parameter vectors we get the quantity

$$Y = \Phi^T \theta \tag{4.8}$$

which for the two respective problems is defined as

$$Y_1 = M_t \left(\frac{\lambda}{s+\lambda} \dot{x}_p - \dot{x}_p\right) + \frac{1}{s+\lambda}\left(A_{p_1} P_1 - A_{p_2} P_s\right) \tag{4.9}$$

and

$$Y_2 = P_1 - \frac{\lambda}{s+\lambda} P_1 \, . \tag{4.10}$$

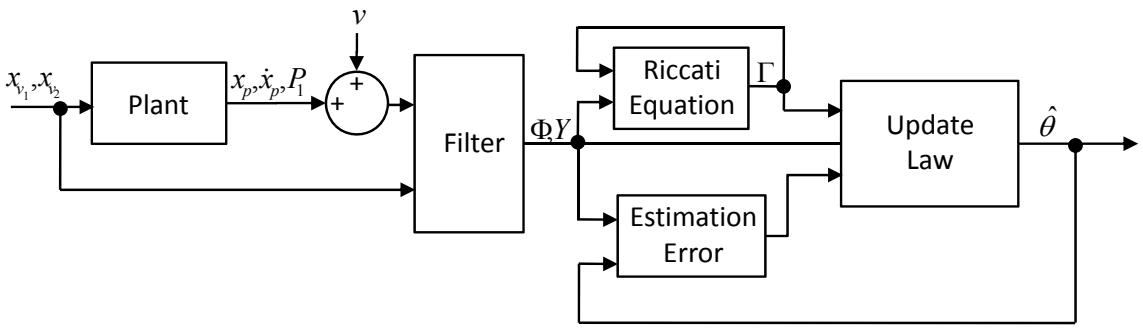

Figure 4.1: Least-Squares Estimator Block Diagram

4.3.1 Least-Squares Update Law

To estimate the parameter vectors, we employ the *unnormalized least-squares with forgetting factor update law* developed in Section 2.3 rewritten for convenience,

$$\dot{\hat{\theta}} = \Gamma\Phi\left(Y - \Phi^T\hat{\theta}\right) \tag{4.11}$$

$$\dot{\Gamma} = \beta\Gamma - \Gamma\Phi\Phi^T\Gamma \tag{4.12}$$

where the equation (4.12) is the Riccati equation for the gain matrix $\Gamma(t)$. An initial condition $\Gamma(0)$ is chosen to be a positive definite and symmetric matrix. β is a design constant which is chosen as $\beta \geq 0$, where $\beta = 0$ makes the algorithm the "pure" least-squares update law. Clearly, for our two parametric models, we employ two identifiers,

$$\dot{\hat{\theta}}_1 = \Gamma_1\Phi_1\left(Y_1 - \Phi_1^T\hat{\theta}_1\right), \quad \dot{\Gamma}_1 = \beta_1\Gamma_1 - \Gamma_1\Phi_1\Phi_1^T\Gamma_1 \tag{4.13}$$

and

$$\dot{\hat{\theta}}_2 = \Gamma_2\Phi_2\left(Y_2 - \Phi_2^T\hat{\theta}_2\right), \quad \dot{\Gamma}_2 = \beta_2\Gamma_2 - \Gamma_2\Phi_2\Phi_2^T\Gamma_2. \tag{4.14}$$

Looking at Figure 4.1 the identifier has four main parts: the filter which provides the values for Φ and Y, the estimation error, the Riccati equation which determines the values for Γ, and the update law which provides the estimate $\hat{\theta}$.

4.3.2 Gradient Update Law

In addition to the least-squares update law we also separately employ the gradient update law developed in Section 2.5 as an alternative to the least-squares method.

$$\dot{\hat{\theta}} = \bar{\Gamma}\Phi\left(Y - \Phi^T\hat{\theta}\right) \tag{4.15}$$

There is no Riccati equation to calculate making this a simpler algorithm to compute. $\bar{\Gamma}$ is chosen to be positive definite and symmetric. However, we seek to incorporate the correlation of the signals. In larger dimensional systems, such as the EHV System, choosing the appropriate correlation values offhand is difficult. Simulating with the least squares algorithm will yield a gain matrix that includes the correlation of all the signals in the system. Therefore $\bar{\Gamma}$ is chosen as the averaged settling value of the gain matrix from the least squares simulation. With our parametric models the gradient identifiers are

$$\dot{\hat{\theta}}_1 = \bar{\Gamma}_1\Phi_1\left(Y_1 - \Phi_1^T\hat{\theta}_1\right), \tag{4.16}$$

and

$$\dot{\hat{\theta}}_2 = \bar{\Gamma}_2\Phi_2\left(Y_2 - \Phi_2^T\hat{\theta}_2\right), \tag{4.17}$$

where $\bar{\Gamma}_1$ and $\bar{\Gamma}_2$ are the averaged settling values of Γ_1 and Γ_2 respectively.

Looking at Figure 4.2 the identifier only has three main parts: the filter which provides the values for Φ and Y, the estimation error, and the update law which provides the estimate $\hat{\theta}$. Since $\bar{\Gamma}$ is static, there is no longer a need for the Riccati equation which updated Γ.

We have shown in Section 2.3 and Section 2.6 that both update laws guarantee that $\hat{\theta}(t)$ converges to the true value θ (in the absence of noise) if the regressor vector $\Phi(t)$ is "persistently exciting." The square-wave character if the input signals in the EHVS application helps ensure persistence of excitation. With persistence of excitation we can choose either the "pure" least-squares algorithm, the least-squares algorithm with forgetting factor, or the gradient algorithm to achieve parameter convergence.

This chapter is in part an adaptation of material as it appears in J. Gray, M. Krstic, N. Chaturvedi, P. Sungbae, A. Kojic, K. Mischker "Parameter Identification for Electrohydaulic Valvetrain Systems," which was submitted to the *ASME Journal*

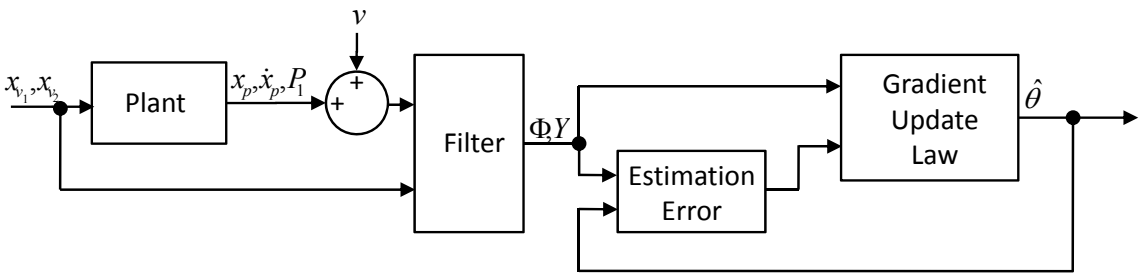

Figure 4.2: Gradient Estimator Block Diagram

of Dynamic Systems, Measurement and Control. The thesis author was the principle researcher and author of this paper.

5

Simulations

5.1 Introduction

With the identifiers defined in Chapter 4 and the system model given in Chapter 3 we can begin simulations of the EHV System. Before simulating the identifiers, we first verify stable system operation and if the signal Φ is PE. Then after ensuring those conditions are fulfilled, we apply the identifiers to the system. We show the convergence properties of the "Pure" least-squares in an idealized case. We then show the improved convergence of the identifier with forgetting factor. After showing parameter convergence in an idealized case, we then corrupt signal inputs for the identifiers with noise and introduce un-modelled dynamics. We also show the various trade-offs in the choice of the forgetting factor. Following this we introduce a hybrid model of the EHV System and compare the system states to the original model. In addition we compare the estimation of the hybrid case in both an ideal case and with noise injected. Finally we show improved estimation performance with a switching identifier on the hybrid system.

5.2 System States

We now present the simulations done of the plant (3.1)-(3.5). In the following simulation, initial conditions were set to be $x_p(0) = 0$, $\dot{x}_p(0) = 0$, and $P_1(0) = \frac{A_{p2}P_s}{A_{p1}}$. The parameter values used in the simulation are given in Table 5.1. These

Table 5.1: Parameter values used in the simulation.

Parameter	**Values**
M_t	1
A_{p1}	20
A_{p2}	10
x_{v1}, x_{v2}	1
V_{01}	5
P_s	250
P_r	10
C_{d1}	10
C_{d2}	10
w_1, w_2	5
ρ	10
B	50
β_e	250
D	6×10^{-9}
D_b	1×10^{-12}
k	5

parameter values differ from the actual system parameter values given by Bosch due to confidentiality issues. However, the values presented were chosen to provide a qualitatively similar system response.

The equations of the plant as given are suitable for when the system is operating within the limits of the device. However, during simulations we have placed a lower saturation limit at $x_p = 0$ because there is a physical stop of the system at that point. Figure 5.1 displays the results from simulations without variable damping (Fig. 5.1 (A)) and with variable damping (Fig. 5.1 (B)). The position of the piston (Fig. 5.13 (A.1)) and velocity (Fig. 5.13 (A.2)) show the necessity for variable damping in the EHV System. The rapid stop creates a hard landing on the valve which will significantly reduce the life-span of the system. Figure 5.13 (B) shows improved closing with variable damping included. The states show the soft seating of the valve is achieved. The impact velocity is greatly reduced before the valve comes to a close.

However, the inclusion of saturation on x_p introduces some model errors. The velocity is reported as negative even when $x_p = 0$ and saturated in Figure 5.1 (A.2).

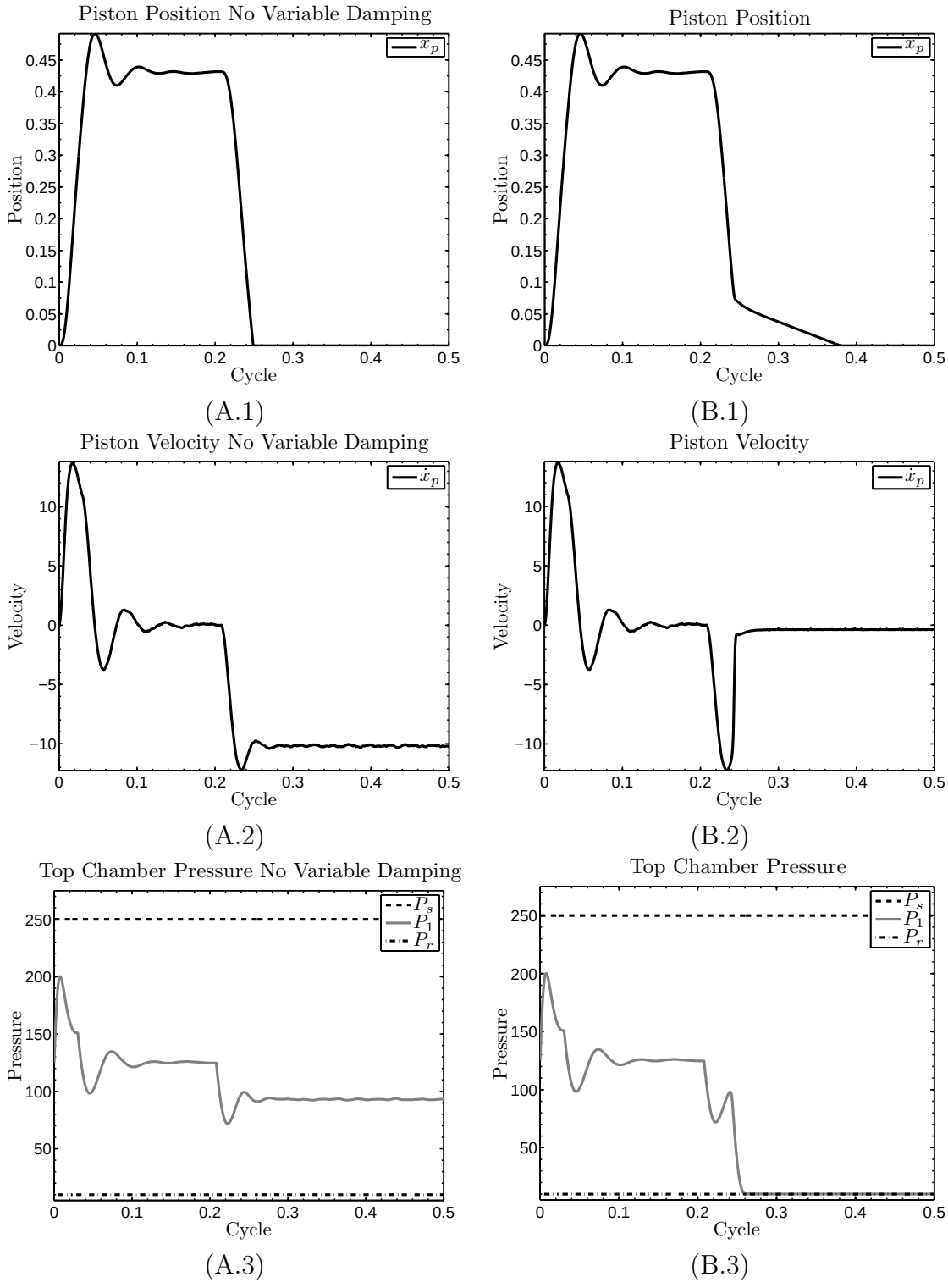

Figure 5.1: Measured system states in transient. (A) No RB (B) RB

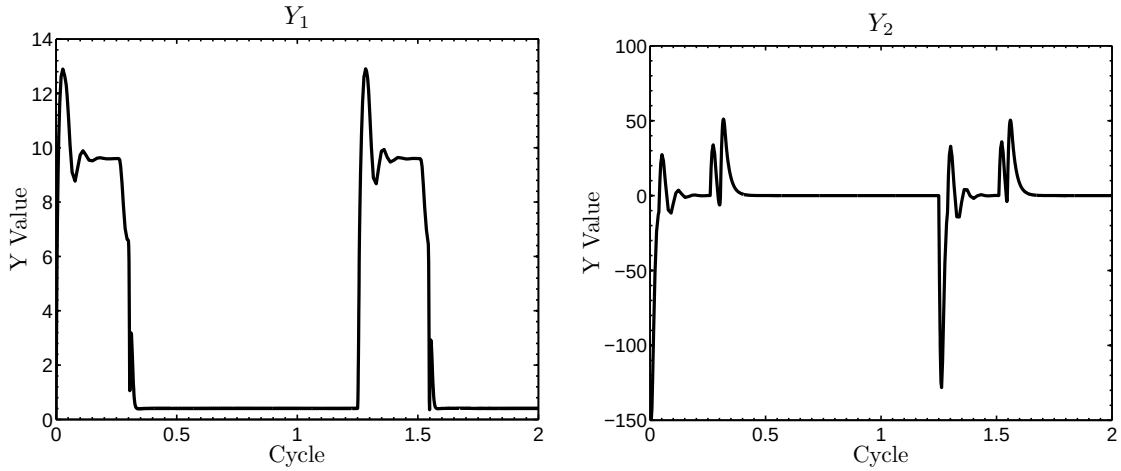

(A) (B)

Figure 5.2: Transients of the identifier quantity Y (A) Y_1 (B) Y_2.

In addition, the pressure in Figure 5.1 (A.3) does not settle to the reservoir pressure (P_r) while x_{v_2} remains open. The variably damped case is a more accurate reflection of the EHV System. While velocity does not settle to a zero value during closing, it is close enough that we will assume this model is still valid.

Another important aspect to verify is the boundedness of the signals Y and Φ. Figure 5.2 displays the values of Y for both subsystems. It appears to be a bounded cyclical measurement that satisfies the earlier assumption of $Y \in \mathcal{L}_\infty$ necessary to insure the cost function $J(\hat{\theta})$ is a convex function. In addition Figure 5.3 shows the values of both regressor vectors Φ_1 and Φ_2. These satisfy $\Phi \in \mathcal{L}_\infty$, completing the other assumption necessary to have $J(\hat{\theta})$ be a convex function of $\hat{\theta}$ over $\mathcal{R}^3$ at each time t.

5.3 Persistence of Excitation

After verifying the stable operation of the system equations (3.1)-(3.5) and confirming the convexity of the cost function $J(\hat{\theta})$, we now move to verify the condition (2.18) for exponential convergence of the identifier. We numerically check if the regressor Φ of each identifier is PE. Taking (2.18) and shifting the bounds of integration

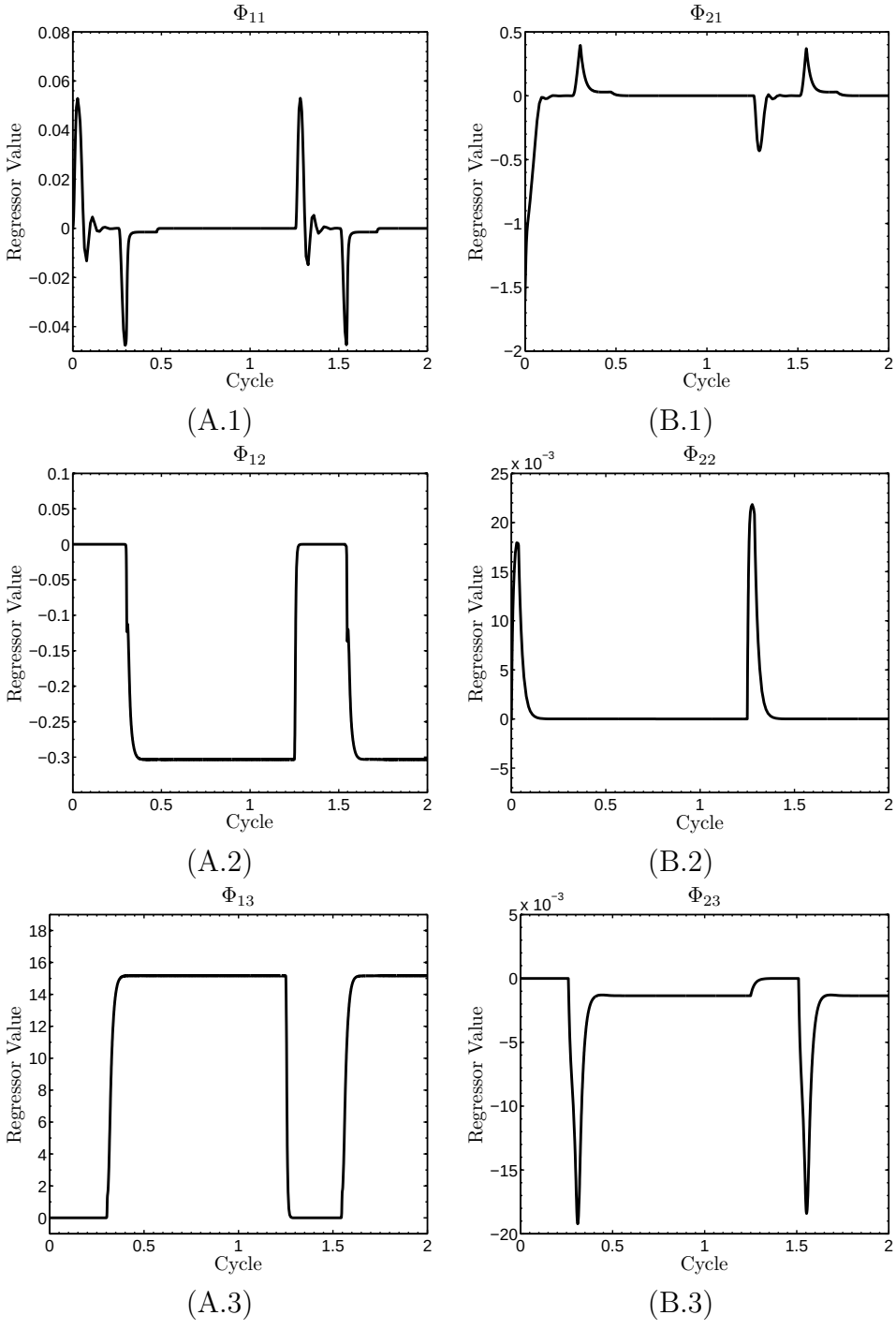

Figure 5.3: Transients of the identifier regressor Φ (A) Φ_1 (B) Φ_2

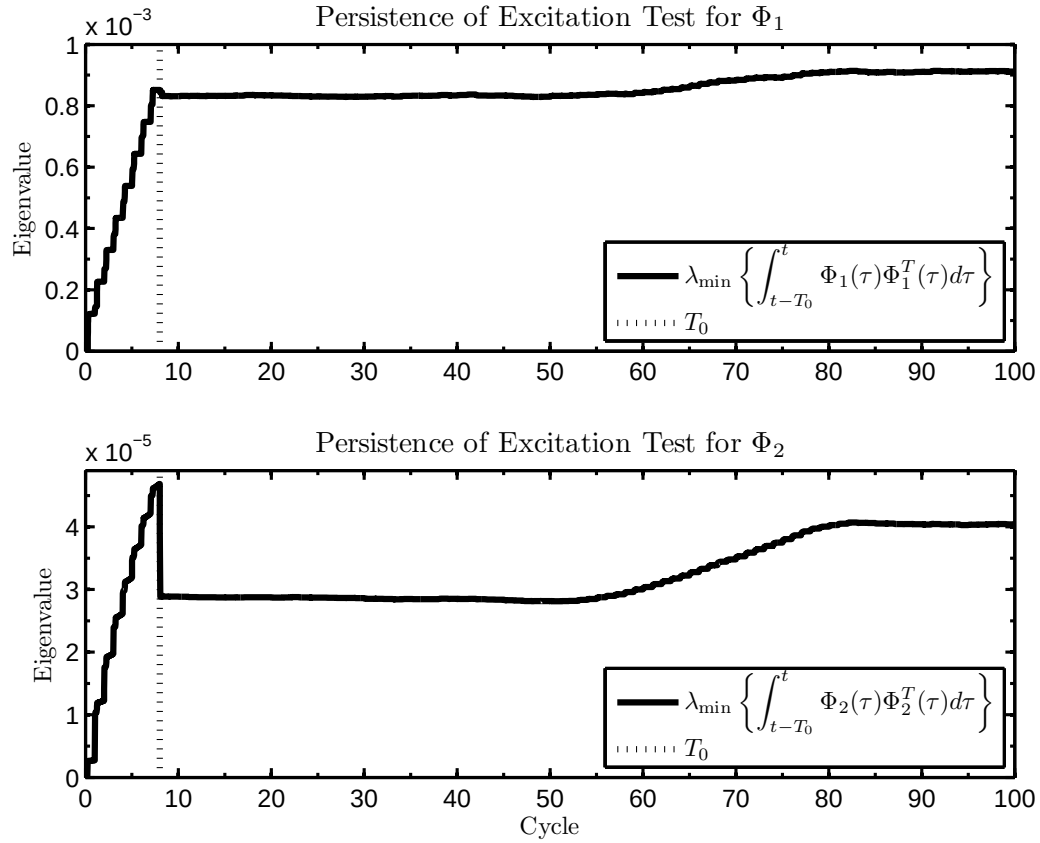

Figure 5.4: Results of the test to determine the PE of the regressors.

results in

$$\frac{1}{T_0}\int_{t-T_0}^{t}\Phi(\tau)\Phi^T(\tau)d\tau \geq \alpha_0 I \tag{5.1}$$

which is satisfied if the following sufficient condition is satisfied:

$$\lambda_{\min}\left\{\int_{t-T_0}^{t}\Phi(\tau)\Phi^T(\tau)d\tau\right\} > 0\,. \tag{5.2}$$

Figure 5.4 contains the result of the numerical simulation of (5.2) with both regressors. Both regressors satisfy the condition of (5.2). Given that PE holds, the identifiers will converge, without forgetting factor polynomially and exponentially in the other cases, to the true parameters in the absence of noise.

5.4 Initial Condition Limitations

After verifying PE and guaranteeing the convergence of the identifier, we begin to employ the various update laws developed in Section 2.3. The regressor vectors Φ_1 and Φ_2 are defined by (4.6) and (4.7) and the quantities Y_1 and Y_2 are defined by (4.9) and (4.10) respectively. In every simulation all true parameters except D and D_b are allowed to vary with time. After forty cycles there is a gradual 20% variation in the true parameters.

Of the various initial estimates only the initial value for the estimate $\hat{D}(0)$ must be chosen with care. Since the regressor vector Φ_1 relies on the estimate $\hat{D}_b$, we take

$$\hat{D}_b = \frac{\hat{D}D_b}{\hat{D}}$$

because the parameter vector (4.4) has no explicit estimate of $\hat{D}_b$. This implies that as $\hat{D}$ approaches 0 the value $\hat{D}_b$ will approach infinity. Therefore if $\hat{D}(0)$ is chosen too small there can be a failure in the identifiers due to division by zero. The same care is not necessary for the initial conditions of other estimates.

5.5 "Pure" Least-Squares Estimation

We will first look at the case of the "Pure" least algorithm described by equations (4.11) and (4.12) with $\beta = 0$ and no noise. Looking at Figure 5.5 shows convergence of the estimator to 5% in about twenty cycles. However problems arise when θ_{11} begins to vary. While $\hat{\theta}_{11}$ (i.e B) continues to adapt to the true parameter, the convergence is at a rate much slower than the system variation. This is evidence of the "covariance wind-up" described in Section 2.3. Figure 5.6 (B) displays the reason behind the slow adaptation. There is a reduction of the gain matrix diagnols by at least two decades within the first twenty cycles. This greatly reduces the ability of the identifier to adjust to variations. In addition, the off-diagonal terms adjust but quickly return back to zero as the estimator achieves convergence. In summary, this may be a good algorithm to use in a static parameter identification, however Figure 5.5 reveals that either a forgetting factor or a constant gain matrix is needed to estimate the dynamic parameters present in this system.

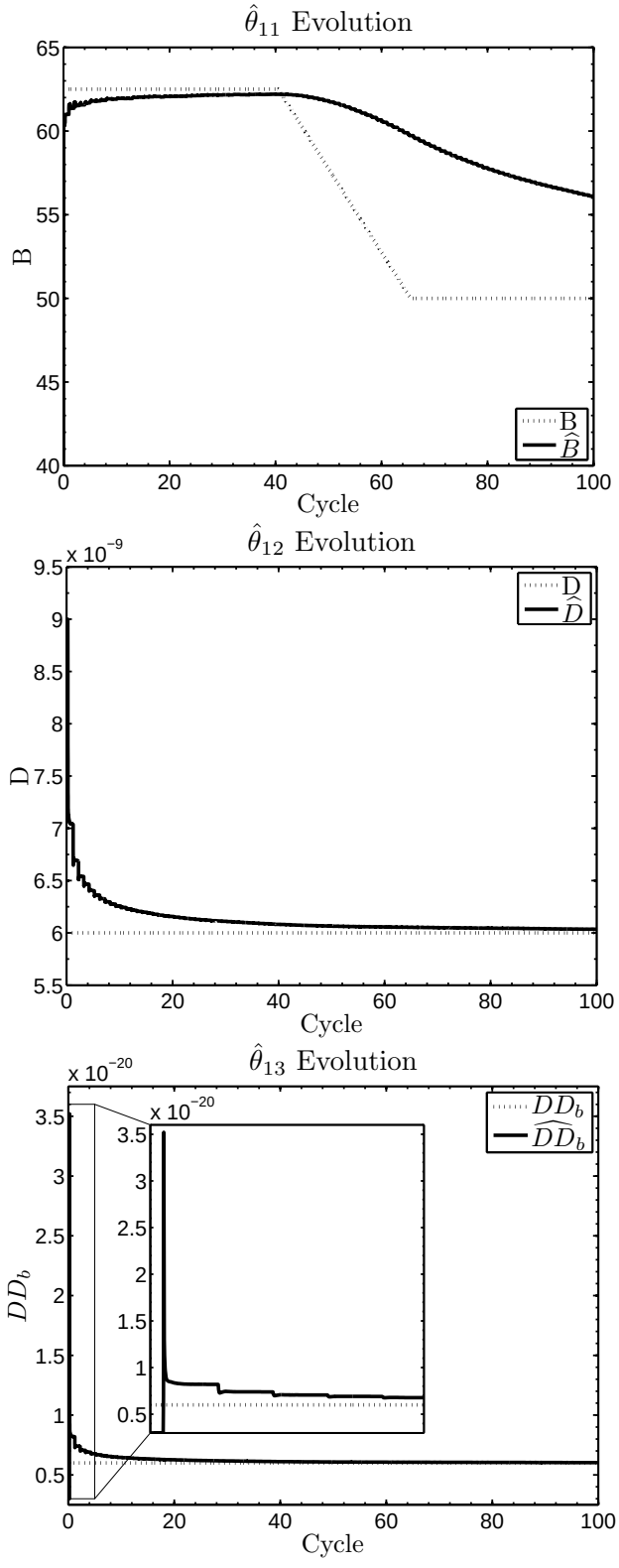

Figure 5.5: Parameter estimation with "Pure" least-squares.

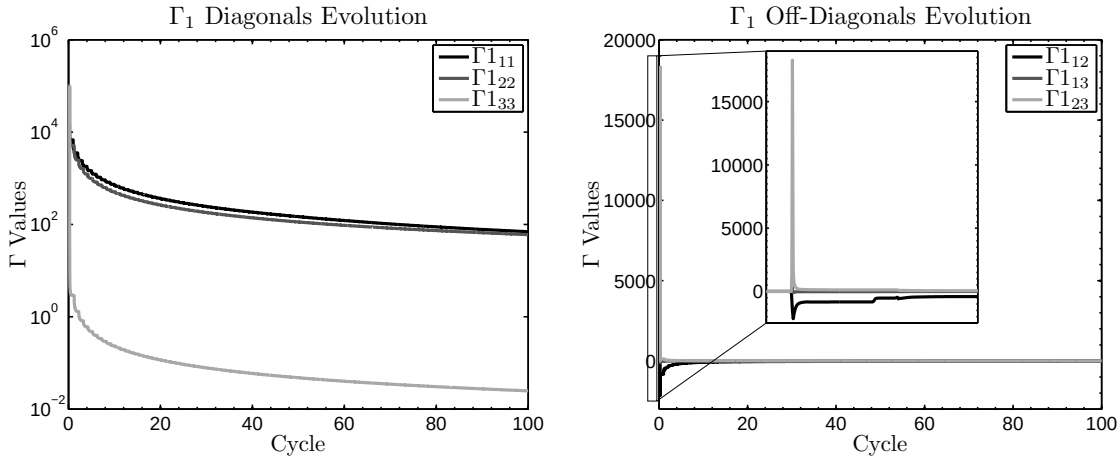

Figure 5.6: "Pure" Γ_1 transient (A) Diagonals (B) Off Diagonals

5.6 Least-Squares with Forgetting Factor Estimation

The second case we will look at is the least-squares algorithm with $\beta > 0$. Looking at a case with no noise in Figure 5.7 we find good parameter estimation with dynamic parameters. Even with the addition of an unknown zero mean force (F_o) being applied in equation (3.1) Figure 5.7 (A) shows the estimate $\hat{\theta}_1$ converging to the true value θ_1 within approximately twenty cycles. When the system parameters change at forty cycles the estimate ($\hat{\theta}_{11}$) continues to adapt and converges to the true value after variation ends. Figure 5.7 (B) displays both a slower convergence rate and a slight downward offset in the estimation. The offset is due to modeling errors in the pressure state, mentioned in Section 5.2. It directly affects the estimate $\hat{\theta}_{23}$ but also slightly propagates through the other estimates in $\hat{\theta}_2$. However, even with the simulation errors, the estimates converge to within 5% of the true value in $\hat{\theta}_{21}$ and $\hat{\theta}_{22}$ and within 10% of the true value in $\hat{\theta}_{23}$.

5.6.1 Examination of the Gain Matrix

The gain of the identifiers show the value of the algorithm's forgetting factor. Figure 5.8 demonstrates the adjustment of gain matrices Γ_1 and Figure 5.9 shows the

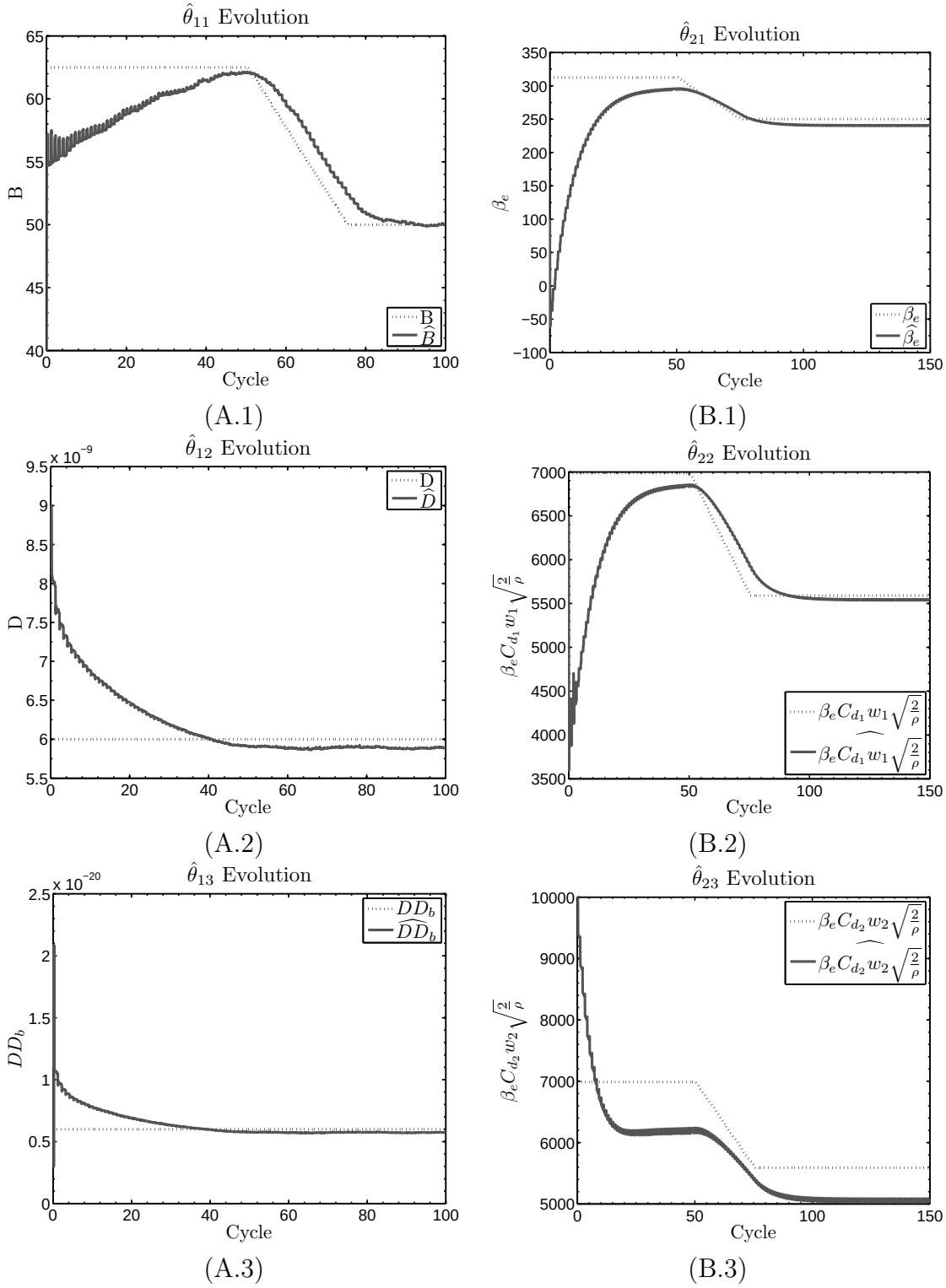

Figure 5.7: No noise estimation of the parameters (A) θ_1 (B) θ_2

adjustments on Γ_2. Both matrices have a period of self-adjustment from the initial condition, after which the values settle to an averaged equilibrium. The off-diagonal terms of the gain matrices grow symmetrically. They self-adjust to the excitation levels of the different channels of the regressor vectors as well. These off-diagonal terms represent the correlation of terms in identifier signals and estimates. For example, in Figure 5.9 the off-diagonal terms in Γ_2 display a high level of correlation. Each estimate ($\hat{\theta}_2$) relies on β_e and each element of the regressor vector Φ_2 relies on measurements of V_1, with two elements (Φ_{22}, Φ_{23}) relying on P_1. There is a similar correlation in θ_1 with every element relying on x_p . After an initial transient (due to poorly chosen initial conditions) the off-diagonal terms of Γ_1 settle to a nonzero value.

5.6.2 Effects of Noise

In addition to the parameter variation, sensor noise is injected into the state measurements which is on the order of 1% of the maximum of the state measurement. Despite these violations of the idealized conditions of the theory (noise and non-constant parameters), most estimates converge to within 5% of the true value within forty cycles. As the true parameters change, the estimates still follow the variation. These results are shown in Figure 5.10 (A) and Figure 5.10 (B).

5.6.3 Forgetting Factor Considerations

We now look at Figure 5.11 to see the trade-off in the choice of the forgetting factor β. A larger β increases the speed of convergence at the cost of an increased sensitivity to noise. Therefore, depending on the tolerance of future controllers, β could be tuned appropriately to allow the quickest convergence while still remaining in tolerance.

In addition to the trade-off in the parameter estimates, Γ is also affected by the choice of β. A larger β will reduce the time it takes Γ to settle into stable oscillations, however a larger β will also increase the mean value of the stable oscillations.

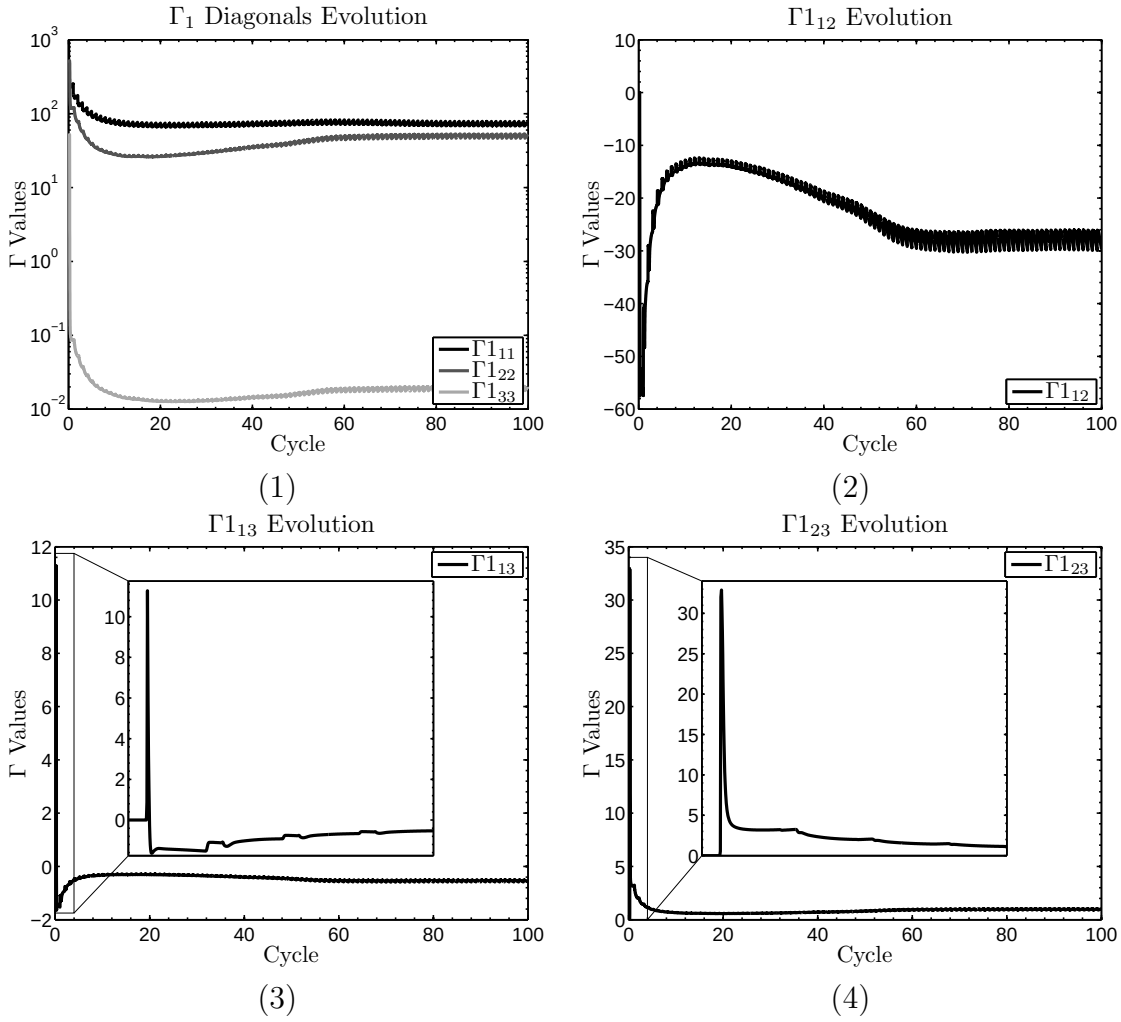

Figure 5.8: Γ_1 evolution on a system with no noise and $\beta > 0$

5.7 Gradient Method

Looking at Figure 5.12 reveals that the gradient method holds many of the same properties of the least-squares algorithm. For instance, even in the presence of system noise and parameter variation the estimate still converges to a value within about 5% of the true value. In certain cases convergence is achieved in fewer cycles with the gradient method. However, the same downward bias that affects the estimates in $\hat{\theta}_2$ with the least-squares algorithm remain present in the gradient algorithm's estimates.

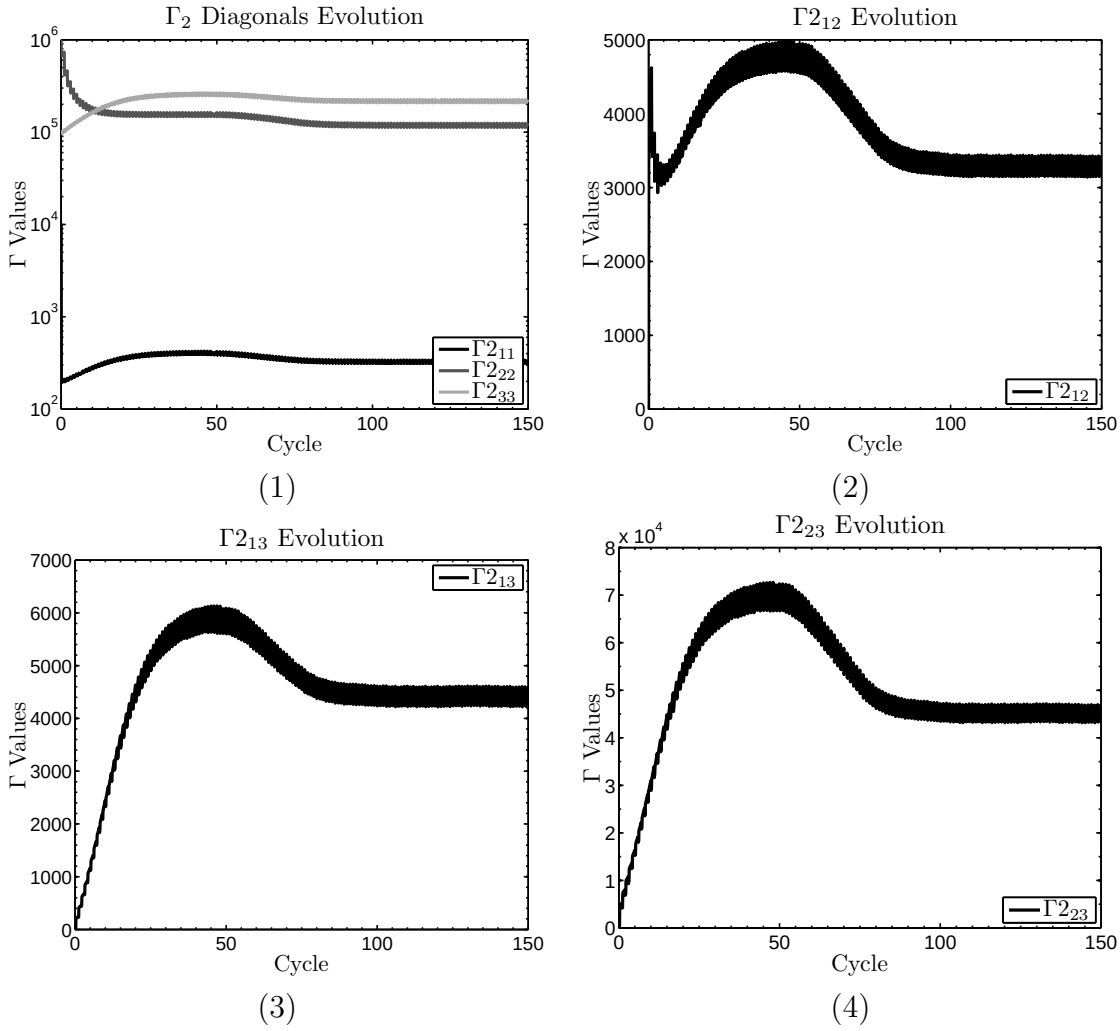

Figure 5.9: Γ_2 evolution on a system with no noise and $\beta > 0$

5.8 Hybrid System

The "Pure" least-squares, least-squares with forgetting factor, and gradient algorithms are estimation methods we explored in these past sections. Of the three, least-squares with forgetting factor and the gradient algorithms were both successful with varying parameters, and also with noisy measurements. While the gradient method is the least computationally complex while still providing equivalent results, it relied on the results from the least-squares algorithm. Without the implementation of the least-squares with forgetting factor algorithm, a gain matrix for the gradient method that included signal correlation would have been difficult to find. After ana-

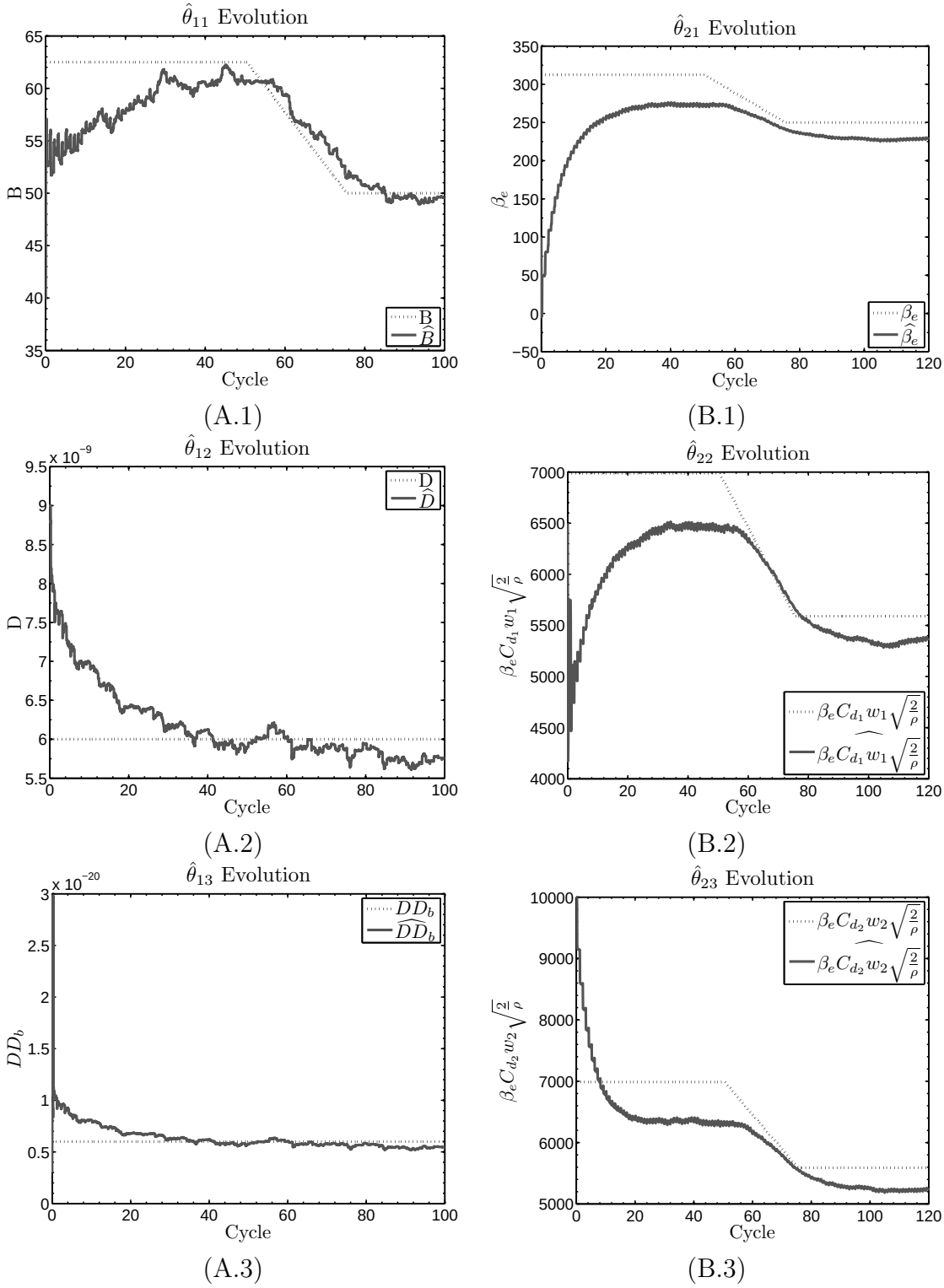

Figure 5.10: Estimation of parameters with noise (A) θ_1 (B) θ_2

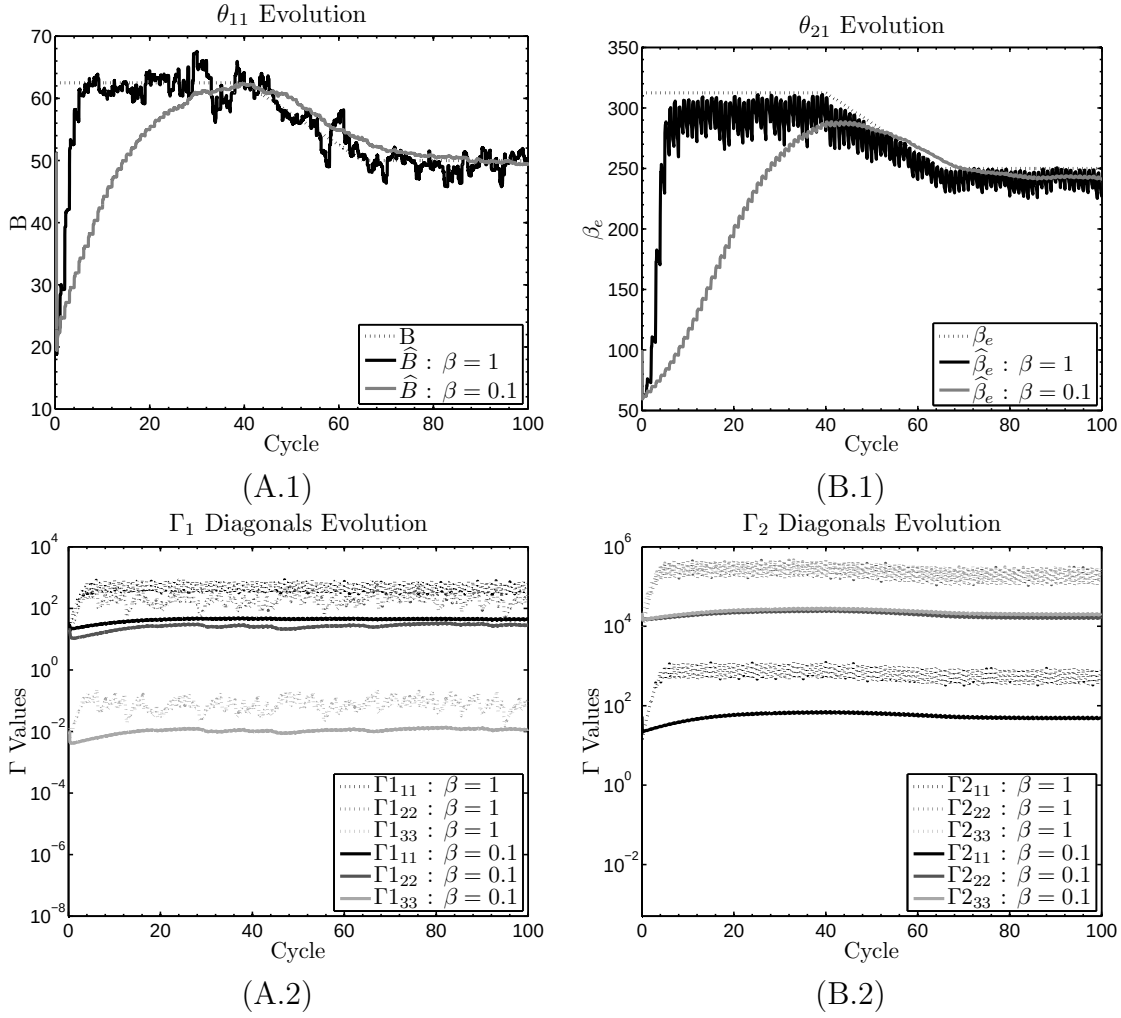

Figure 5.11: Forgetting factor's effect on estimation and gains. (A) Piston Subsystem (B) Pressure Subsystem

lyzing the methods and showing convergence of the estimates, we now move to include un-modelled dynamics into the system such with a hybridization of the system.

As mentioned in Section 5.2 the non-hybrid case shows that a lower saturation limit on x_p does not propagate the correct response through the other states $\dot{x}_p$ and P_1. To address this issue and more accurately represent the actual physical system's behavior we will modify the plant differential equations. We take the following hybrid

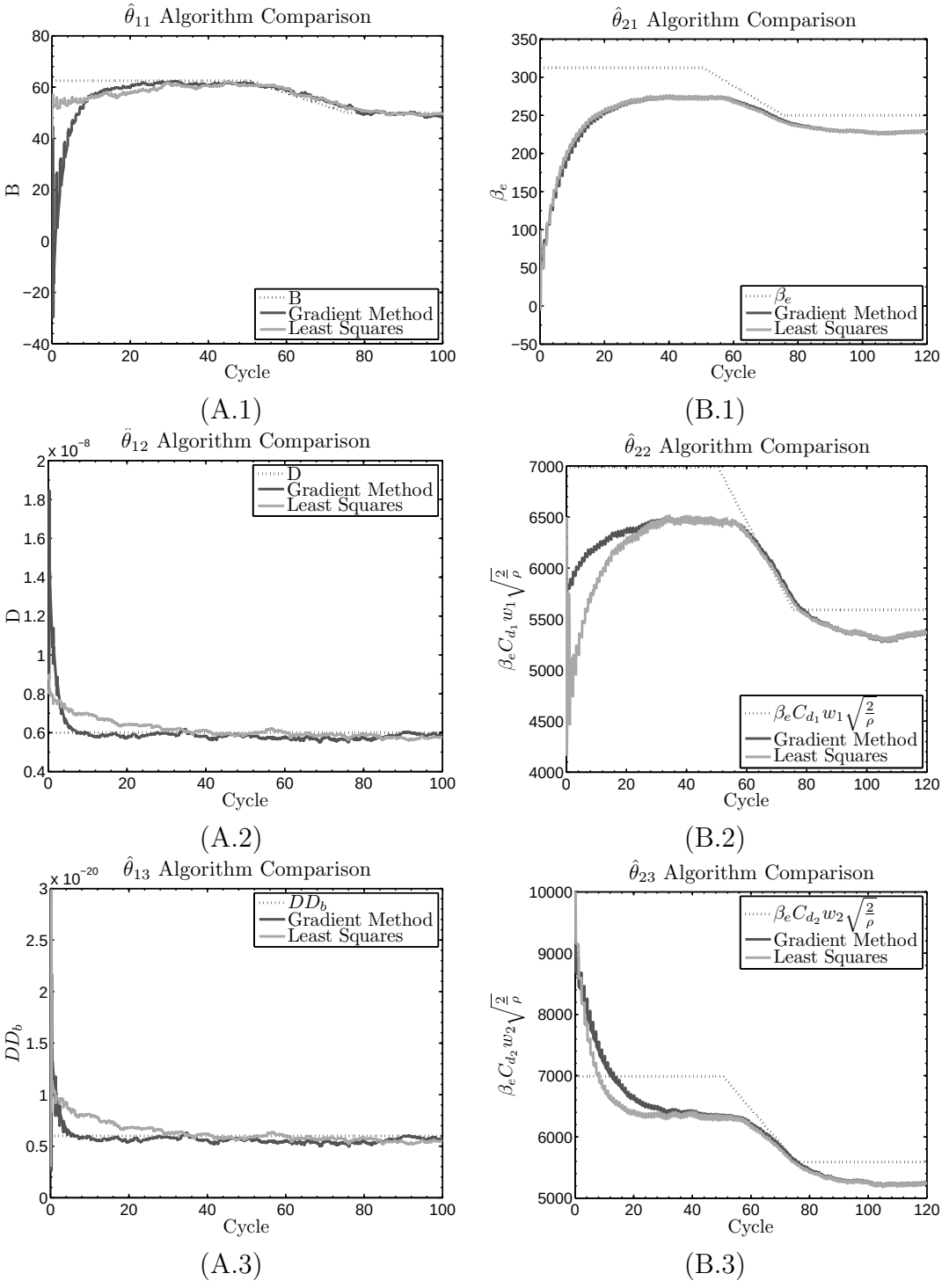

Figure 5.12: Least-squares compared to the gradient method (A) θ_1 (B) θ_2

model,

$$
\begin{aligned}
&\textbf{If } \{x_p > 0\} \\
&\qquad M_t\ddot{x}_p = A_{p_1}P_1 - A_{p_2}P_s - F_o - B\dot{x}_p - RB \\
&\qquad \dot{V}_1 + \frac{V_1}{\beta_e}\dot{P}_1 = Q_1 - Q_2 \\
&\textbf{If } \{x_p = 0\} \quad x_p^+ = 0,\, \dot{x}_p^+ = 0,\, P_1 = P_r \\
&\qquad \textbf{If } \{\ddot{x}_p < 0\} \\
&\qquad\quad M_t\ddot{x}_p = M_t\ddot{x}_p \\
&\qquad\quad \frac{V_1}{\beta_e}\dot{P}_1 = Q_1 \\
&\qquad \textbf{If } \{\ddot{x}_p \geq 0\} \\
&\qquad\quad M_t\ddot{x}_p = A_{p_1}P_1 - A_{p_2}P_s - F_o \\
&\qquad\quad \frac{V_1}{\beta_e}\dot{P}_1 = Q_1\,.
\end{aligned}
\tag{5.3}
$$

This set of equations has three different cases. The first case is original plant presented in Chapter 3. In the second case the valve is closed and the valve housing is acting in an equal and opposite direction of the piston. There is no velocity and the chamber pressure is exhausted to the reservoir pressure. In the true system the top chamber pressure chamber will eventually reach reservoir pressure if x_{v2} is open. However in simulations not setting $P_1 = P_r$ at closing requires a prohibitively small time step to reflect that dynamic. So in simulation P_1 is set to P_r when x_p hits zero in the hybrid system. The final case is when there is enough pressure to force the valve open. After the opening the valve returns to the original plant.

5.8.1 State Comparison

Figure 5.13 (A) is a non-variably damped direct comparison of the original plant (3.1)-(3.5) to the new hybrid system, equation (5.3). From this it is clear that hybrid system better reflects actual system behavior. As expected, the initial behavior is identical in both systems. When the valve closes the differences in both velocity and pressure appear. As discussed before, the velocity is reported as negative even when $x_p = 0$ and saturated in Figure 5.13 (A.2) in the non-hybrid case. In addition, the

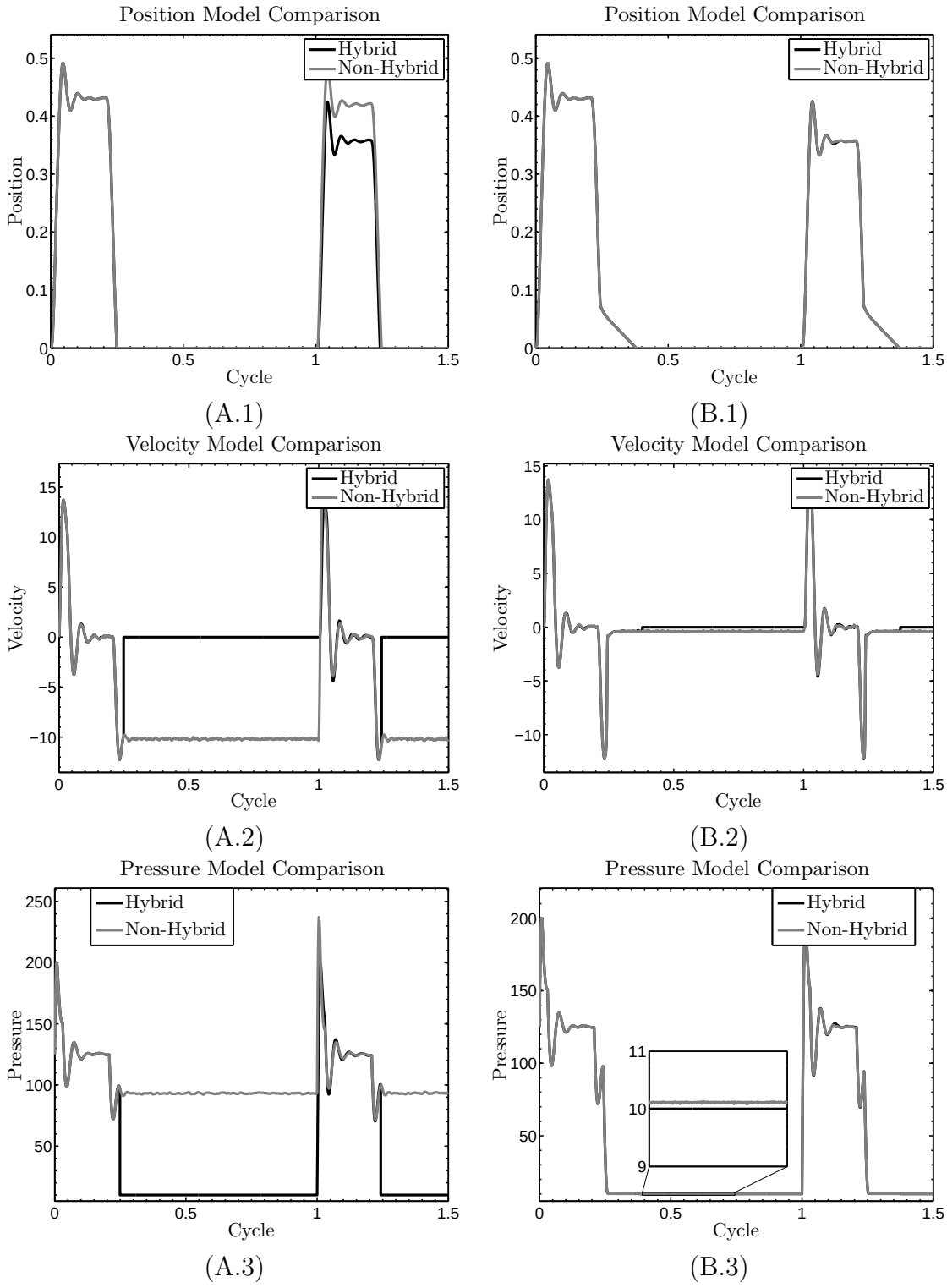

Figure 5.13: A comparison of system models. (A) without RB (B) with RB

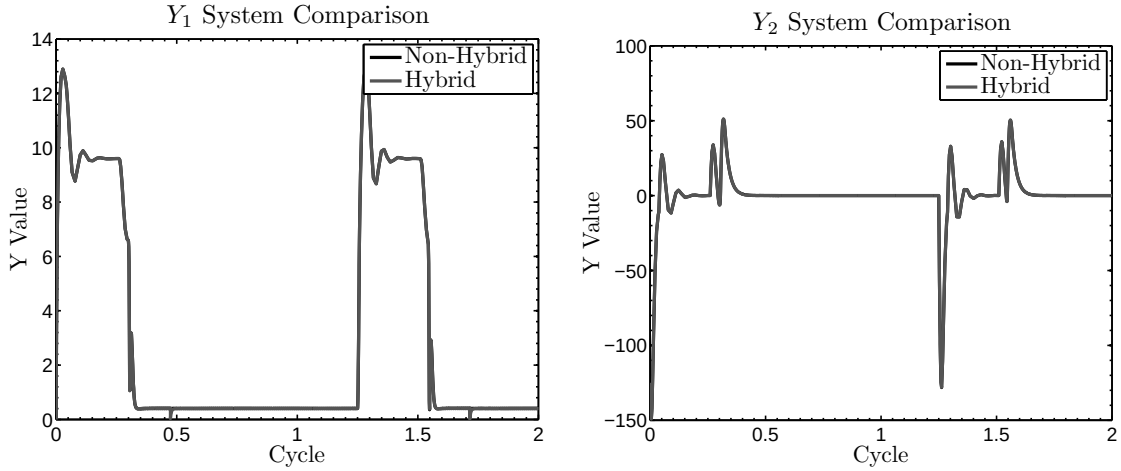

Figure 5.14: Modelling effects on the quantity Y. (A) Y_1 (B) Y_2.

difference of the intermediate velocity and pressure values changes the transient of x_p in the second cycle.

Looking at Figure 5.13 (B) the main differences between the two system models is in the velocity Figure 5.13 (B.2) and pressure states Figure 5.13 (B.3). At 0.4 cycles the hybrid velocity is set to zero, whereas the non-hybrid system remains at a small non-zero constant. Looking at the inset on Figure 5.13 (B.3) the pressure shows another slight difference, with P_1 settling to P_r only in the hybrid case. From Figure 5.13 it is clear that the hybrid model is a more accurate physical model of the EHV System.

5.8.2 Identifier Comparison

Changing the model also has the potential to change the identifiers. To see the effects of the changes on the identifiers we compare the differences on the various regressor vectors and Y quantities. The graphs in Figure 5.14 shows a direct comparison of the quantities Y_1 (Fig. 5.14 (A)) and Y_2 (Fig. 5.14 (B)) of the two models. Figure 5.15 shows the comparison of the behavior of regressors Φ_1 (Fig. 5.15 (A)) and Φ_2 (Fig. 5.15 (B)) of the two representations. The velocity and pressure difference cause Φ_{12} (Figure 5.15 (A.2)), Φ_{13} (Fig. 5.15 (A.3)), and Φ_{23} (Fig. 5.15 (B.3)) to differ in the two representations. The difference between the two system representations

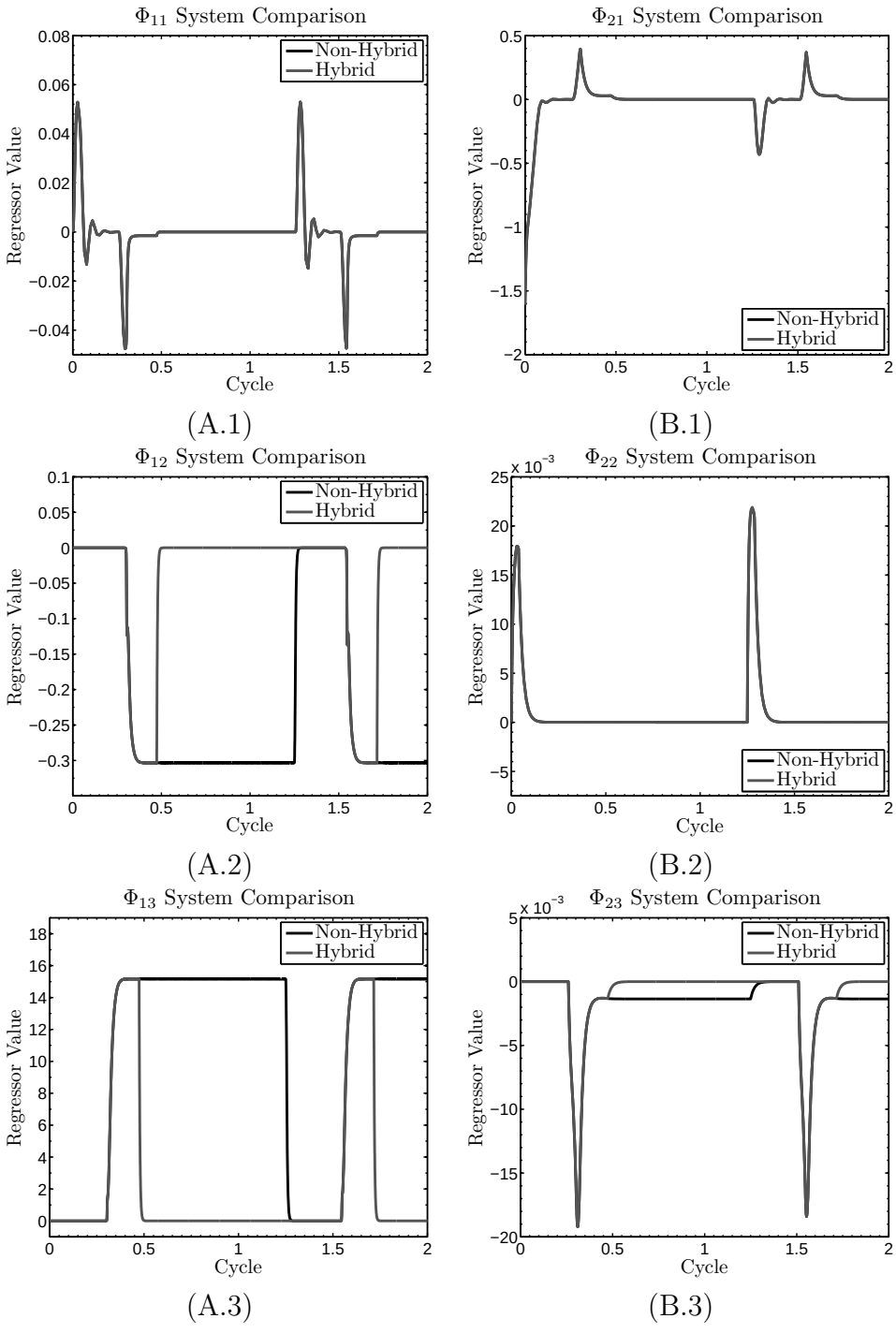

Figure 5.15: Modelling effects on the regressor Φ. (A) Φ_1 (B) Φ_2

is mainly in the duration of excitation of Φ_{12}, Φ_{13}, and Φ_{23}. Since this is the case, we assume that the regressors will still drive $\Phi^T\hat{\theta}$ to the quantity Y in the hybrid representation without any identifier modifications. Looking at the actual values of Y_1 and Y_2 in Figure 5.14 we find that they same in both hybrid and non-hybrid representations. Because of these facts, we assume that the identifiers will drive the estimates to the true parameters.

5.9 Estimation of the Hybrid System

We now present the results of parameter estimation on the hybrid system developed in Section 5.8. We examine the case of no sensor noise using the least square with forgetting factor algorithm given in equations (4.11) and (4.12). Looking at a direct comparison of the estimation with no noise, other then the zero mean force (F_o), we find that the convergence is improved on hybrid system. Figure 5.16 (A) shows the estimation of the piston subsystem is relatively unchanged, however Figure 5.16 (B) displays an improvement in the estimation on the pressure subsystem. There is no longer a downward bias on the estimation of θ_2. The bias stems from the downward velocity affecting equation (3.2) the hybrid representation removes.

5.9.1 Effects of Noise

We now look at the effects of noise on the hybrid system estimation. The improvement in estimation in the ideal case is not realized when noise is injected into sensor measurements. The noise on states x_p and $\dot{x}_p$ must be reduced by an order of magnitude to provide reliable estimates of the system. Noise mainly effects the piston subsystem, but after the reduction of noise Figure 5.17 (A) shows strong convergence properties with a slight downward bias. The estimation of θ_2 (Fig. 5.17 (B)) in the hybrid case with noisy inputs is similar to the non-hybrid case with a downward bias returning to the estimate.

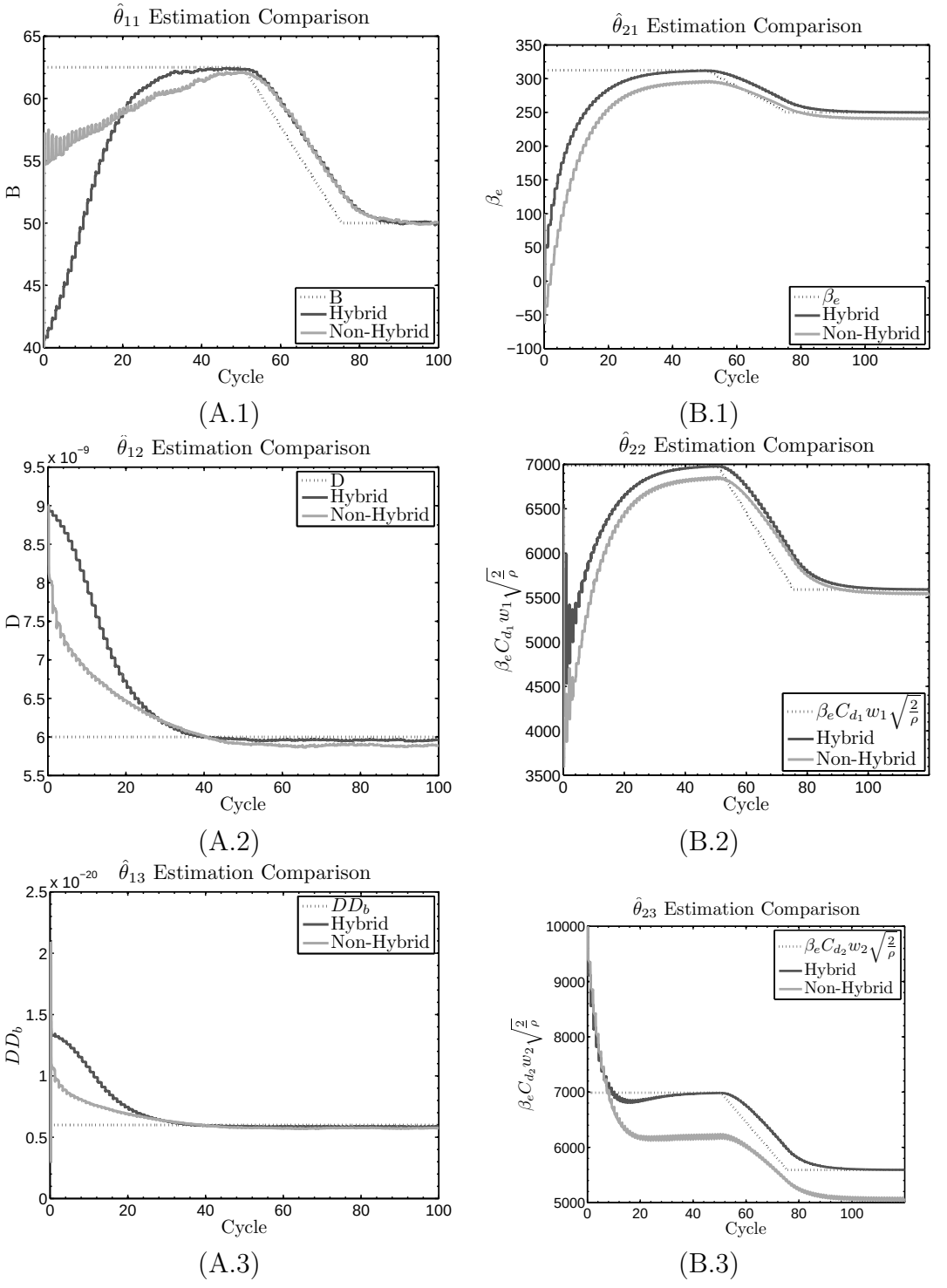

Figure 5.16: Estimation comparison of the two models (A) θ_1 (B) θ_2

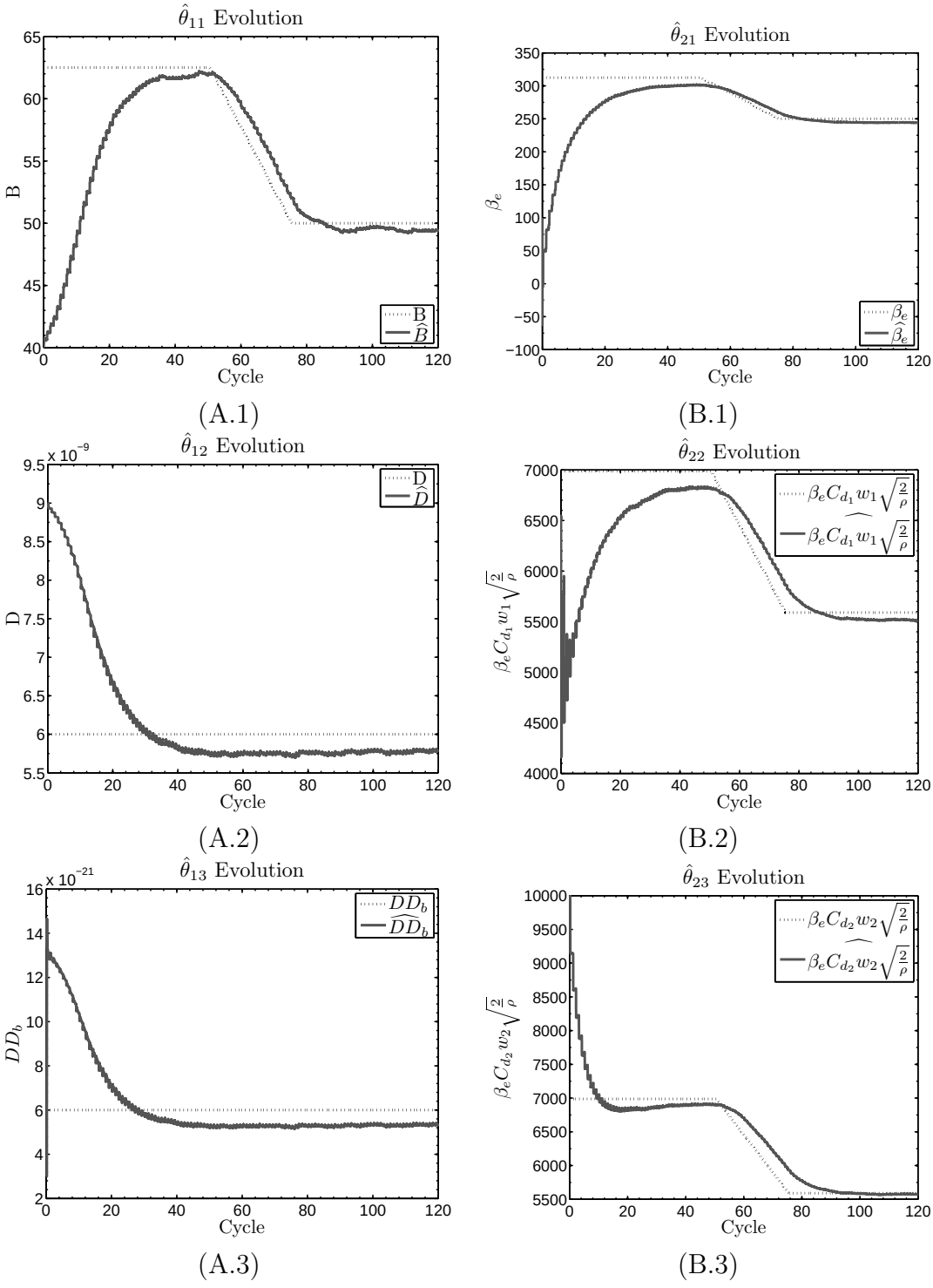

Figure 5.17: Estimation of the hybrid system with noise (A) θ_1 (B) θ_2

5.9.2 Switching Least-Squares Identifier

We modified the estimation scheme to accommodate the same levels of noise as the non-hybrid system estimation. Since the main differences between the hybrid and non-hybrid systems arise when x_p is closed, we turn off estimation when x_p is closed. We modify the least-squares algorithm as follows:

$$\begin{aligned} &\textbf{If } \{x_p > 0\} \\ &\qquad \dot{\hat{\theta}} = \Gamma\Phi\left(Y - \Phi^T\hat{\theta}\right) \\ &\qquad \dot{\Gamma} = \beta\Gamma - \Gamma\Phi\Phi^T\Gamma \\ &\textbf{If } \{x_p = 0\} \\ &\qquad \dot{\hat{\theta}} = 0\,. \end{aligned} \tag{5.4}$$

This allows for adaptation only when the system matches the identifier model, as opposed to trying to identify parameters when there is both an incorrect model and only noisy activity. Figure 5.18 compares the results of this switching identifier on the hybrid system to the original identifier on the non-hybrid representation. Both identifiers have the same noise levels on the sensors. While estimates of θ_1 (Fig. 5.18) are similar, estimates of θ_2 (Fig. 5.18) show an improvement in convergence to the true value.

This chapter is in part an adaptation of material as it appears in J. Gray, M. Krstic, N. Chaturvedi, P. Sungbae, A. Kojic, K. Mischker "Parameter Identification for Electrohydaulic Valvetrain Systems," which was submitted to the *ASME Journal of Dynamic Systems, Measurement and Control*. The thesis author was the principle researcher and author of this paper.

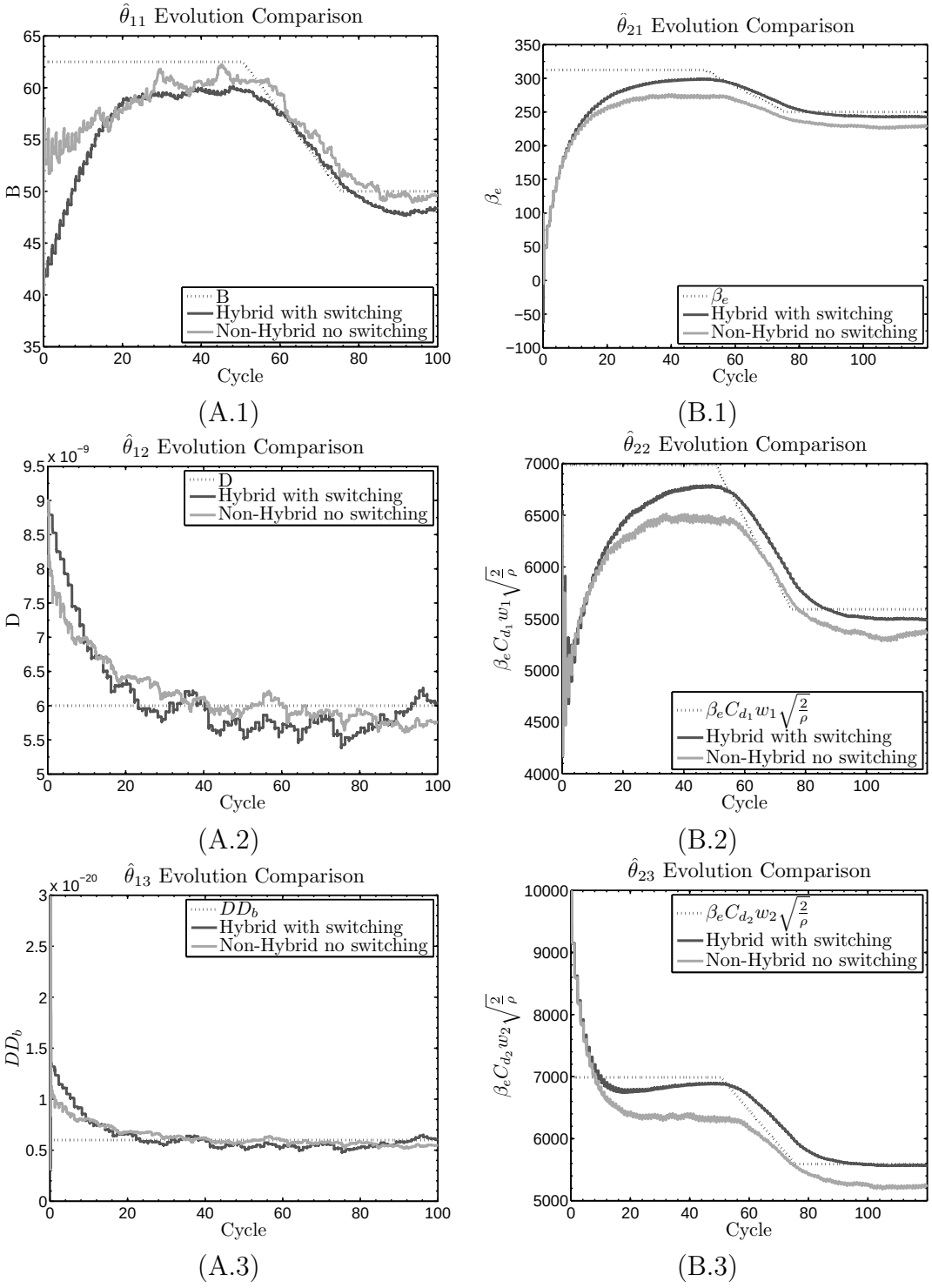

Figure 5.18: Comparison of switching and original identifiers (A) θ_1 (B) θ_2

6

Conclusion

6.1 Summary of Findings in this Thesis

The objective of this thesis is to design an online parameter identifier of an EHV System in the presence of varying parameters. While designing the estimator, we consider three algorithms and test their effectiveness in simulation. The results show strong convergence properties which will be useful in future controls work on the system.

The underlying theory of the identifiers are presented in Chapter 2. We introduce the process of creating a linear parametric model of the system which is important for the identifier design. After we develop the base functions of the least-squares algorithms and prove convergence of both the "Pure" least-squares algorithm and the least-squares with forgetting factor. Lastly we develop and prove exponential convergence of the gradient algorithm. However, it is shown that PE of the input signal is a necessity for convergence.

The modeling of the EHV System in Chapter 3 is important. We created a physics based model of the system. In addition a model for the variable damping mechanism was developed. That model was non-linear in an unknown parameter so in order to achieve a linear parametric model we created a Taylor approximation of the variable damping model. With this approximation we could represent the EHV System in a linear parametric model.

The identifier for the EHV System was created in Chapter 4. A linear parametric

model is created from the EHV System. The regressors, Φ, and quantities Y of the identifiers are created from the EHV System's two differential equations. The least-squares and gradient update laws were introduced.

The EHV System and the identifiers are then simulated in Chapter 5. Stable system operation and PE of the system was first tested to insure convergence. We found that with varying parameter a "Pure" least-squares algorithm is insufficient for identification. Least-squares with forgetting factor achieved convergence, though it was biased in the presence of noise. We applied a gradient identifier using the averaged gains of the least-squares algorithm as gain matrix. This exhibited similar properties to the least squares algorithm while being less computationally complex.

Lastly we looked at the identifier's performance on a hybrid model in Section 5.8. We found that with the original least-squares identifier parameter convergence occurs. However, the convergence is more sensitive to noise. To remove some model identifier discrepancies we simulated a switching least-squares identifier which turns off adaptation when the valve is closed. The switching least-squares identifier estimating the hybrid system has similar convergence properties to the least-squares identifier estimating the non-hybrid system.

6.2 Future Work

The contents of this thesis represent the first step towards the goal of an adaptive EHVS controller. The work presented here is a summary of tasks to be completed to implement a successful controller.

6.2.1 Refine Variable Damping Model

This thesis provides one mathematical model of the variable damping present in the EHVS. This method can be used to create approximations of the system, which must be matched to experimental results. While this may be good for one setup, it may vary with different configurations of the variable damping system.

An option to this is to create a physics based model of the variable damping system. This may introduce hybrid dynamics in the model which may complicate

the identifier. However this will make the actual model more accurate especially if the variable damping varies during operation. It is of interest to find if the more complicated model is necessary. It may be that the mathematical model is sufficient for control purposes.

6.2.2 Reduce Sensors

As of now the inputs necessary for the identifiers include a pressure sensor, a velocity sensor, and a position sensor. Each sensor adds an expense which will make the EHV System cost prohibitive to implement on a wide scale. The velocity sensors are mainly used in terms Φ_{12}, Φ_{13}, and Y_1. In Y_1, $\dot{x}_p$ appears linearly, however in Φ_{12} and Φ_{13} it appears with an absolute value. There is a possibility that using a second order stable filter on the valve piston subsystem and approximating valve closing can eliminate the need for a velocity sensor. The removal of the pressure sensor poses a more difficult problem. However, if possible the identifier could then be realized with only a position sensor. This would greatly increase the viability of the EHV System as it would considerably reduce costs associated with sensors.

6.2.3 Control Design

Looking at literature there are many benefits to having a valve system that is fully decoupled from the engine camshaft. However, it must be able to reliably open and close valves through many varying engine events such as acceleration and idling. After creating a control algorithm for the EHV System timing and valve lift can then be tuned to optimize the operation of the engine. For instance, an extremum-seeking based algorithm could measure emission output of the engine and actively tune the valves to reduce overall emissions. Then a variety of options could be analyzed to create the optimum valve profiles for engine operation.

It is left to future persons involved with this project to determine the control design of the EHV System.

Bibliography

[1] A. Alleyne and J. K. Hedrick, "Nonlinear adaptive control of active suspensions," *IEEE Transactions on Control Systems Technology*, vol. 3, pp. 94–101, 1995.

[2] A. Alleyne and R. Liu, "A simplified approach to force control for electro-hydraulic systems," *Control Engineering Practice*, vol. 8, pp. 1347–1356, 2000.

[3] J. S. Brader and D. N. Rocheleau, "Development of a piezoelectrically-controlled hyraulic actuator for a camless engine. Part 1: system design," *Proceedings of the Institution of Mechanical Engineers*, vol. 218, pp. 817–822, 2004.

[4] R. R. Chladny and C. R. Koch, "Flatness-based tracking of an electromechanical variable valve timing actuator with disturbance observer feedforward compensation," *IEEE Transactions on Control Systems Technology*, vol. 16, no. 4, pp. 652–663, 2008.

[5] R. R. Chladny, C. R. Koch, and A. F. Lynch, "Modeling automotive gas-exchange solenoid valve actuators," *IEEE Transactions on Magnetics*, vol. 41, no. 3, pp. 1155–1162, 2005.

[6] S. B. da Cuhna, J. K. Hedrick, and A. P. Pisano, "Variable valve timing by means of a hydraulic actuation," no. 2000-01-1220, 2000.

[7] D. Denger and K. Mischker, "The electro-hydraulic valvetrain system EHVS-system and potential," ser. SAE Technical paper, no. 2005-01-0774, SAE World Congress, Detroit, USA, 2005.

[8] P. Eyabi and G. Washington, "Modeling and sensorless control of an electromagnetic valve actuator," *Mechatronics*, vol. 16, pp. 159–175, 2006.

[9] P. M. FitzSimons and J. J. Palazzolo, "Part 1: modeling of a one-degreee-of-freedom active hydraulic mount," *ASME Journal of Dynamic Systems, Measurements, and Control*, vol. 118, no. 3, pp. 439–442, 1996.

[10] G. Fontana and E. Galloni, "Variable valve timing for fuel economy improvement in a small spark-ignition engine," *Applied Energy*, vol. 86, pp. 96–105, 2009.

[11] W. Hoffmann, K. Peterson, and A. G. Stefanopoulou, "Iterative learning control for soft landing of electromechanical valve actuator in camless engines," *IEEE Transactions on Control Systems Technology*, vol. 11, no. 2, pp. 174–184, 2003.

[12] P. A. Ioannou and J. Sun, *Robust Adaptive Control*. Prentice Hall, 1996.

[13] J. Kim and J. Chang, "A new electromagnetic linear actuator for quick latching," *IEEE Transactions on Magnetics*, vol. 43, no. 4, pp. 1849–1852, 2007.

[14] J. Ma, G. Zhu, A. Hartsig, and H. Schock, "Model-based predictive control of an electro-pneumatic exhaust valve for internal combustion engines," in *American Control Conference, 2008*, 2008.

[15] M. Montanari, F. Ronchi, C. Rossi, and A. Tonielli, "Control of a camless engine electromechanical actuator: position reconstruction and dynamic performance analysis," *IEEE Transactions on industrial electronics*, vol. 51, no. 2, pp. 299–311, 2004.

[16] K. Nagaya, H. Kobayashi, and K. Koike, "Valve timing and valve lift control mechanism for engines," *Mechatronics*, vol. 16, pp. 121–129, 2006.

[17] N. Niksefat and N. Sepehri, "Design and experimental evaluation of a robust force controller for an electro-hydraulic actuator via quantitative feedback theory," *Control Engineering Practice*, vol. 8, pp. 1335–1345, 2000.

[18] M. Pachter, C. H. Houpis, and K. Kang, "Modelling and control of an electro-hydrostatic actuator," *International Journal of Robust and Nonlinear Control*, vol. 7, pp. 591–608, 1997.

[19] T. A. Parlikar, W. S. Chang, Y. H. Qiu, M. D. Seeman, D. J. Perreault, J. G. Kassakian, and T. A. Keim, "Design and experimental implementation of an electromagnetic engine valve drive," *IEEE/ASME Transactions on Mechatronics*, vol. 10, no. 5, pp. 482–493, 2005.

[20] K. S. Peterson and A. G. Stefanopoulou, "Extremum seeking control for soft landing of an electromechanical valve actuator," *Automatica*, vol. 40, pp. 1063–1069, 2004.

[21] M. Pischinger, W. Salber, F. V. D. Staay, H. Baumgarten, and H. Kemper, "Low fuel consumption and low emissions- electromechanical valve train in vehicle operation," *International Journal of Automotive Technology*, vol. 1, no. 1, pp. 17–25, 2000.

[22] J. Pohl, M. Sethson, P. Krus, and J. Palmberg, "Modeling and validation of a fast switching valve intended for combustion engine valve trains," *Proceedings of the Institution of Mechanical Engineers, Part 1: Journal of Systems and Control Engineering*, vol. 216, no. 2, pp. 105–212, 2002.

[23] D. Popović, M. Janković, S. Magner, and A. R. Teel, "Extremum seeking methods for optimization of variable cam timing engine operation," *IEEE Transactions on Control Systems Technology*, vol. 14, no. 3, pp. 398–407, 2006.

[24] C. Tai, T.-C. Tsao, and M. B. Levin, "Adaptive nonlinear feedforward control of an electrohydraulic camless valvetrain," in *American Control Conference, 2000*, 2000.

[25] G. Vossoughi and M. Donath, "Dynamic feedback linearization for electrohydraulically actuated control systems," *ASME Journal of Dynamic Systems, Measurement, and Control*, vol. 117, no. 4, pp. 468–477, 1995.

[26] Y. Wang, T. Megli, M. Haghgooie, K. S. Peterson, and A. G. Stefanopoulou, "Modeling and control of electromechanical valve actuator," *SAE 2002-01-1106*, 2002.

[27] B. Yao, F. Bu, J. Reedy, and G. T. Chiu, "Adaptive robust motion control of single-rod hydraulic actuators: theory and experiments," *IEEE/ASME Transactions on Mechatronics*, vol. 5, no. 1, pp. 79–91, 2000.

[28] H. Yu, Z. jin Feng, and X. yong Wang, "Nonlinear control for a class of hydraulic servo system," *Journal of Zhejiang University Science*, vol. 5, no. 11, pp. 1413–1417, 2003.

[29] J. Yu, C. Zhaoneng, and Y. Lu, "The variation of oil effective bulk modulus with pressure in hydraulic systems," *ASME Journal of Dynamic Systems, Measurement, and Control*, vol. 116, pp. 146–150, 1994.